Persoonia 50, 2023: 27–47
www.ingentaconnect.com/content/nhn/pimj

RESEARCH ARTICLE

ISSN (Online) 1878-9080
https://doi.org/10.3767/persoonia.2023.50.02

Wild rodents harbour high diversity of *Arthroderma*

Š. Moulíková[1,2], M. Kolařík[2], J.M. Lorch[3], D. Kolarczyková[1], V. Hubka[1,2], A. Čmoková[2]

Key words

Arthroderma
geophilic dermatophytes
GlobalFungi
mating type genes
new taxa
polyphasic taxonomy
wild rodents

Abstract *Arthroderma* is the most diverse genus of dermatophytes, and its natural reservoir is considered to be soil enriched by keratin sources. During a study on the diversity of dermatophytes in wild small rodents in the Czech Republic, we isolated several strains of *Arthroderma*. To explore the diversity and ecological significance of these isolates from rodents (n = 29), we characterised the strains genetically (i.e., sequenced ITS, *tubb* and *tef1α*), morphologically, physiologically, and by conducting mating experiments. We then compared the rodent-derived strains to existing ITS sequence data from GenBank and the GlobalFungi Database to further investigate biogeography and the association of *Arthroderma* species with different types of environments. In total, eight *Arthroderma* species were isolated from rodents, including four previously described species (*A. crocatum*, *A. cuniculi*, *A. curreyi*, *A. quadrifidum*) and four new species proposed herein, i.e., *A. rodenticum*, *A. simile*, *A. zoogenum* and *A. psychrophilum*. The geographical distribution of these newly described species was not restricted to the Czech Republic nor rodents. Additional isolates were obtained from bats and other mammals, reptiles, and soil from Europe, North America, and Asia. Data mining showed that the genus has a diverse ecology, with some lineages occurring relatively frequently in soil, whereas others appeared to be more closely associated with live animals, as we observed in *A. rodenticum*. Low numbers of sequence reads ascribed to *Arthroderma* in soil show that the genus is rare in this environment, which supports the hypothesis that *Arthroderma* spp. are not soil generalists but rather strongly associated with animals and keratin debris. This is the first study to utilise existing metabarcoding data to assess biogeographical, ecological, and diversity patterns in dermatophytes.

Citation: Moulíková Š, Kolařík M, Lorch JM, et al. 2022. Wild rodents harbour high diversity of Arthroderma. Persoonia 50: 27–47. https://doi.org/10.3767/persoonia.2023.50.02.
Effectively published online: 1 February 2023 [Received: 6 April 2022; Accepted: 1 November 2022].

INTRODUCTION

Dermatophytes (*Ascomycota: Onygenales*) are keratinophilic fungi studied mainly due to the pathogenicity of some species. Dermatophytes in human and domestic animals are of high scientific and medical interest whereas those associated with wild animals are less well-studied. However, small wild mammals are known to be reservoirs of diverse dermatophyte species, including those capable of infecting humans and domestic animals (Mantovani 1978, Hubálek et al. 1979, Hubálek 2000). In particular, wild rodents are occasional hosts of *Trichophyton mentagrophytes* and *T. quinckeanum*, two species with significant zoonotic potential (Menges et al. 1957, McKeever et al. 1958, Mantovani et al. 1982, Gallo et al. 2005, Papini et al. 2008, Chollet et al. 2015, Uhrlaß et al. 2018, Lysková et al. 2021). Wild rodents (e.g., North American porcupine, *Erethizon dorsatus*) are also known to be natural reservoirs of emerging pathogens from the *T. benhamiae* complex (Needle et al. 2019, Čmoková et al. 2020). Fungal infections contracted from wild animals are uncommon, perhaps because direct contact is rare. However, infections contracted from contaminated environments (such as soil) have been more frequently described (Umnova & Fomenko 1960, Chmel et al. 1967, 1975, Moretti et al. 2013).

A substantial number of dermatophytes isolated from rodents belong to the genus *Arthroderma* (Mantovani et al. 1982, Chabasse et al. 1987, Gallo et al. 2005, Papini et al. 2008), which also represents the most diverse genus of dermatophytes. Recently, several novel species were described (Brasch & Gräser 2005, Hubka et al. 2015, Lorch et al. 2015, Brasch et al. 2019, Hainsworth et al. 2021) and phylogenetic relationships in the genus were resolved by Hainsworth et al. (2021).

Soil is widely considered to be the natural reservoir of fungi in the genus *Arthroderma* (De Hoog et al. 2017, Hainsworth et al. 2021). However, *Arthroderma* species are frequently isolated from hairs, nests, and burrows of animals and occasionally from human clinical material as well (Dawson 1963, Hubálek et al. 1979, Hubka et al. 2014a, Hainsworth et al. 2021). The degree to which *Arthroderma* flourishes in soil in the absence of animal-derived keratin is unknown. The importance of the soil environment as a habitat for these fungi was experimentally investigated by testing their ability to actively grow in unsterilised soil (Pugh 1964, Ibbotson & Pugh 1975). However, investigated strains showed rather low competitiveness in the soil environment containing other soil microorganisms (Pugh 1964). Furthermore, the genus is rarely recovered from soil samples (Grin & Ožegović 1963, Chabasse et al. 1987, Hamm et al. 2020). Taken together, these findings indicate that *Arthroderma*

[1] Department of Botany, Faculty of Science, Charles University, Prague, Czech Republic.
[2] Laboratory of Fungal Genetics and Metabolism, Institute of Microbiology of the Czech Academy of Sciences, Prague, Czech Republic; corresponding author e-mail: cmokova@gmail.com.
[3] U.S. Geological Survey — National Wildlife Health Center, Madison, Wisconsin, USA.

species are not soil generalists but rather fungi closely associated with animals and their surrounding environments. The pathogenic potential, although frequently discussed (Brasch & Gräser 2005, Nenoff et al. 2014, Brasch et al. 2019), is controversial and poorly understood for *Arthroderma*. A notable exception is the species *A. redellii*, which causes skin infections in hibernating bats (Lorch et al. 2015). Thus, the debate is ongoing about the role of *Arthroderma* species as soil fungi, keratin-dependant commensals or pathogens.

Knowledge about geographical distribution and host affinity of *Arthroderma* species would be valuable in understanding their ecological niches. Zoophilic dermatophytes have complex geographic distributions that mirror those of their hosts (Hubka et al. 2018, Čmoková et al. 2020, 2021). In contrast, soil fungal generalists might be expected to be more widely distributed and limited primarily by climatic and soil parameters (e.g., acidity, moisture) and less by other factors (e.g., plant communities, dispersal barriers) generally affecting the distribution of soil fungi (Gams 2007, Větrovský et al. 2019).

Research of geographic distribution patterns of fungi has traditionally relied on cultivation-based studies but is increasingly complemented with molecular data mining approaches. Public nucleotide sequence databases such as NCBI GenBank (Sayers et al. 2019) and UNITE (Nilsson et al. 2019) enable searching (BLASTn search) against fungal barcodes generated by Sanger technology. Recently, the GlobalFungi Database tool (Větrovský et al. 2020) was introduced to enable searching against millions of sequences generated from massively parallel (next generation) sequencing technologies. Such tools and datasets provide a means by which to study dermatophyte species distribution and habitat affiliations. Specifically, soil is one of the most abundant substrates represented in the GlobalFungi Database and offers an opportunity to test the hypothesis that *Arthroderma* species are ubiquitously distributed in soil rather than being closely associated with animal hosts.

In this study, we aimed to 1) survey *Arthroderma* diversity associated with wild rodents in the Czech Republic; 2) determine the substrate affinity and geography of newly proposed species by comparing them with published fungal datasets from environmental samples; and 3) expand this bioinformatics survey to the entire *Arthroderma* genus, to better understand the ecology, diversity, and biogeography of the genus. We aimed to compare diversity detected in environmental DNA data obtained through next generation sequencing (mostly from soil and plant material) with those recovered by traditional approaches (e.g., cultivation of isolates) from various sources. This is the first study on dermatophyte diversity, ecology, and geography conducted using data mining of environmental DNA data.

MATERIALS AND METHODS

Source of isolates

Individuals of three rodent species: house mouse (*Mus musculus*), yellow-necked mouse (*Apodemus flavicollis*), and bank vole (*Myodes glareolus*) were captured in Longworth live traps (Flowerdew et al. 2004) at several localities in the Czech Republic during 2019 (Matějková et al. 2020, Moudra et al. 2021). These rodent species differ in the amount of contact they have with humans. Bank voles are an exoanthropic species, living in wild areas and having little contact with humans; yellow-necked mice are a hemisynanthropic species that often live in proximity to humans and may have occasional contact with humans; and house mice are an eusynanthropic species, frequently occupying human abodes (Chmel et al. 1975). Material for isolation of fungi was acquired by brushing the fur of the rodent on the dorsal and ventral surfaces of the body and on the head using a sterile toothbrush or a sterile flocked swab FLOQSwabs (Copan, Murrieta, CA, USA). Collected material was stored in individual sterile plastic bags at -20 °C.

Ethical standards

All animal procedures were carried out in strict accordance with the law of the Czech Republic paragraph 17 no. 246/1992. This study was, in accordance with accreditation no. 27335/2013-1721 and no. 13060/2014-MZE-17214, approved by the local ethics committee of the Faculty of Science, Charles University in Prague chaired by Stanislav Vybíral, Ph.D.

Isolation

Material collected from rodents was inoculated onto Sabouraud dextrose agar (SDA; HiMedia, Mumbai, India) with antibiotics (500 mg/L cycloheximide, 40 mg/L chloramphenicol) and incubated at 25 °C, 30 °C, and 37 °C. Petri dishes were incubated for 1 month and morphotypically distinct colonies were isolated using malt extract agar (MEA; HiMedia, Mumbai, India) to isolate individual clones. Pure isolates were cultivated at 25 °C and dermatophyte strains were identified based on a combination of molecular and phenotypic methods. Isolates were deposited into the Culture Collection of Fungi (CCF), Department of Botany, Charles University, Prague, Czech Republic; dried herbarium specimens were deposited into the herbarium of the Mycological Department, National Museum in Prague, Czech Republic (PRM).

Molecular studies

DNA was extracted from colonies using the DNeasy UltraClean Microbial Kit (Qiagen, Hilden, Germany) following manufacturer's instructions. The ITS rDNA region was amplified using forward primer ITS1F and reverse primers ITS4 or NL4 (White et al. 1990, Gardes & Bruns 1993, O'Donnell 1993); a portion of the *tubb* gene, encoding β-tubulin, and portion of the *tef1α* gene, encoding translation elongation factor 1-α, were amplified using primers Bt2a and Bt2b (Glass & Donaldson 1995) and EF-DermF and EF-DermR (Mirhendi et al. 2015), respectively. Newly designed primers were used for the amplification of mating-type gene idiomorphs. Primers ART-MAT1F1 and ART-MAT1R1 were developed to amplify a portion of the MAT1-1-1 gene and primers ART-MAT2F1 and ART-MAT2R1 were developed to amplify MAT1-2-1. All primer combinations are listed in Appendix 1. Each 20-µL reaction contained 1 µL (50 ng) of DNA, 0.3 µL of each primer (25 µM), 0.2 µL of MyTaq Polymerase, and 4 µL of 5 × MyTaq PCR buffer (Bioline, London, UK). PCR conditions and PCR product purification was conducted as described by Sklenář et al. (2021). Automated sequencing was performed using the respective forward and reverse primers at Microsynth (Balgach, Switzerland). Sequences were inspected and assembled using BioEdit v. 7.2.6 (Hall 1999). All DNA sequences were deposited into the GenBank database; accession numbers are listed in Table 1.

Phylogenetic analysis

Alignments of the ITS rDNA, *tubb* and *tef1α* loci were performed using the online tool MAFFT v. 7 (Katoh et al. 2019). Alignments were trimmed and concatenated using the online tool Fasta alignment joiner (Villesen 2007), then analysed using maximum likelihood (ML) and Bayesian inference (BI) analyses.

A suitable partitioning scheme and substitution models (Bayesian information criterion) for analyses were selected using the greedy strategy implemented in PartitionFinder 2 with settings allowing introns and exons as independent partitions (Lanfear et al. 2017). The optimal partitioning scheme for ML analysis divided the dataset into six partitions with the following substitution

Table 1 List of *Arthroderma* strains examined in this study.

Species	Culture collection numbers[1,2,3]	Provenance	GenBank/ENA/DDBJ accession numbers[4]		
			ITS	*tubb*	*tef1α*
Arthroderma amazonicum	CBS 967.68 = ATCC 18393^{T}	Brazil, Amazonas, Manaus, hair of rat (*Oryzomys*), *D. Borelli*	LR136967	LR136780	LR136781
	CBS 221.75 = ATCC 28356 = IHEM 3454 = CDC Y-81 = RV 34870	Brazil, near Belém and Guama river, hair of spiny rat (*Proechimys guayanensis*), *A.A. Padhye*	LR136966	LR136778	LR136779
Arthroderma chiloniense	CBS 144073 = DSM 106167 = CCF 6188^{T}	Germany, Kiel, skin of 68-year-old woman	LT992885	LR702008	LR702009
Arthroderma ciferrii	CBS 272.66 = UAMH 2534^{T}	USA, Arkansas, soil, *L. Ajello*	AJ007844	HF937403	LR136782
Arthroderma crocatum	IHEM 5251 = CCF 5300 = ATCC 66309 = NHL 2986 = UAMH 6331^{T}	Japan, Hokkaido, Nakagawa-cho, Nakagawa-gun, soil, 1986, *H. Kubo*	LR136969	LR136785	LR136786
	CBS 130.70	The Netherlands, Oostelijk Flevoland, soil, 1969, *J.H. van Emden*	LR136968	LR136783	LR136784
	CCF 6388	Czech Republic, forest near Sedlečko (Karlovy Vary), fur of *Myodes glareolus*, 2019, *Š. Moulíková*	**OM568940**	**OM677689**	**OM568825**
	CCF 6438	Czech Republic, forest near Sedlečko (Karlovy Vary), fur of *Myodes glareolus*, 2019, *Š. Moulíková*	**OM568941**	**OM677690**	**OM568826**
Arthroderma cuniculi	CBS 492.71 = ATCC 28442 = IHEM 4437 = IMI 096244^{MT}	UK, Scotland, soil from rabbit burrows and rabbit hair, *C.O. Dawson*	KT155926	LR136787	LR136788
	CBS 495.71 = ATCC 18444 = IMI 096245^{MT}	UK, Scotland, soil from rabbit burrows and rabbit hair, *C.O. Dawson*	MH860233	LR136789	LR136790
	CGS12-1	Czech Republic, forest near Sedlečko (Karlovy Vary), fur of *Myodes glareolus*, 2019, *Š. Moulíková*	**OM568942**	**OM677691**	**OM568827**
Arthroderma curreyi	CBS 353.66^{T}	UK, dune soil, 1966, *A.E. Apinis*	LR136970	LR136791	LR136792
	CCF 6386	Czech Republic, forest near Sedlečko (Karlovy Vary), fur of *Myodes glareolus*, 2019, *Š. Moulíková*	**OM568943**	**OM677692**	**OM568828**
	CGS13-3	Czech Republic, forest near Sedlečko (Karlovy Vary), fur of *Myodes glareolus*, 2019, *Š. Moulíková*	**OM568944**	**OM677693**	**OM568829**
Arthroderma eboreum	CBS 117155 = DSM 16978^{T}	Germany, man skin (patient born in the Ivory Coast), 2004, *J. Brasch*	LR136971	LR136793	LR136794
Arthroderma flavescens	CBS 473.78 = IMI 117341^{T}	Australia, Queensland, feather of sacred kingfisher (*Halycon sancta*), 1965, *R.G. Rees*	LR136972	LR136795	LR136796
Arthroderma gertleri	UAMH 2620^{T}	Germany, soil, *H. Böhme*	LR136973	LR136797	LR136798
	CBS 665.77 = UAMH 2819 = CDC X-848	Unknown, *L. Ajello*	LR136963	LR136772	LR136773
Arthroderma gloriae	CBS 663.77 = ATCC 16658 = UAMH 2821^{MT}	USA, Arizona, soil, *L. Ajello*	AJ877209	LR136799	LR136800
	CBS 664.77 = ATCC 16657 = UAMH 2820^{MT}	USA, Arizona, soil, *L. Ajello*	LR136974	LR136801	LR136802
Arthroderma insingulare	UAMH 3438^{MT}	Canada, Alberta, Edmonton, Alberta Game Farm, soil, 1968, *A.A. Padhye*	LR136975	LR136803	LR702007
	UAMH 3440^{MT}	Canada, Alberta, Fort Macleod, chicken feathers, 1968, *A.A. Padhye*	LR136976	LR136804	LR136805
	BY 3809	USA, bedroom carpet, 2016, *Z. Jurjević*	**OM568923**	**OM677674**	–
	CBS 521.71 = UAMH 3441 = ATCC 22519 = IMI 158873	The result of mating between strains UAMH 3438 and UAMH 3440	**OM568924**	**OM677675**	**OM568809**
	CBS 522.71 = UAMH 3442 = ATCC 22520 = IMI 158874	The result of mating between strains UAMH 3438 and UAMH 3440	**OM568925**	**OM677676**	**OM568810**
	CCF 5417 = D 331_15	Czech Republic, České Budějovice, woman 65 years, right toenail, 2015, *N. Mallátová*	**OM568926**	**OM677677**	**OM568811**
	CCF 5938 = 24230-02 dorsal skin #1 I2	USA, Vermont, Rutland County, skin of *Crotalus horridus*, coll. *D. Blodgett* 2009, isol. *J.M. Lorch* 2013	**OM568927**	**OM677678**	**OM568812**
	CCF 5939 = NWHC 24411-01 skin I2	USA, Massachusetts, Middlesex County, skin of *Lampropeltis triangulum*, 2013, coll. *J. Marzolf*, isol. *J.M. Lorch*	**OM568928**	**OM677679**	**OM568813**
	CCF 5940 = NWHC 24411-01 skin I3	USA, Massachusetts, Middlesex County, skin of *Lampropeltis triangulum*, 2013, coll. *J. Marzolf*, isol. *J.M. Lorch*	**OM568929**	**OM677680**	**OM568814**
	CCF 5941 = NWHC 24825-01 skin I2-DTM	USA, Massachusetts, Norfolk County, skin of *Crotalus horridus*, 2014, coll. *A. Stengle*, isol. *J.M. Lorch*	**OM568930**	**OM677681**	**OM568815**
	CCF 5942 = NWHC 44736-22-snout-I1	USA, New Jersey, Morris County, skin of *Coluber constrictor*, 2013, coll. *K. Mitchell*, isol. *J.M. Lorch*	**OM568931**	**OM677682**	**OM568816**
	CCF 5943 = NWHC 44797-157-I1-DTM	USA, Alabama, Conecuh County, wing skin of hibernating bat (*Myotis austroriparius*), 2015, coll. *N. Sharp*, isol. *J.M. Lorch*	**OM568932**	**OM677683**	**OM568817**
	CCF 5944 = NWHC 45692-17-shed-I1-DTM	UK, Essex, Epping Forest, skin of *Natrix natrix*, coll. *L. Franklinos* 2014, isol. *J.M. Lorch* 2016	**OM568933**	**OM677684**	**OM568818**
	SK 1555_16	Czech Republic, Prague, woman 53 years, toenail, 2016, *M. Skořepová*	**OM568934**	**OM677685**	**OM568819**
	UAMH 754	Canada, Alberta, Edmonton, horse pasture, 1959, *J.W. Carmichael*	**OM568935**	**OM677686**	**OM568820**
	UAMH 2922	Hungary, soil, 1962, *S. Szathmary*	**OM568936**	–	**OM568821**
	UAMH 2923	Hungary, soil, 1962, *S. Szathmary*	**OM568937**	–	**OM568822**
	UAMH 2925	USA, California, soil, unknown	**OM568938**	**OM677687**	**OM568823**
	UAMH 3439	Canada, Alberta, Edmonton, Alberta Game Farm, soil, 1968, *A.A. Padhye*	**OM568939**	**OM677688**	**OM568824**
Arthroderma lenticulare	CBS 307.65 = ATCC 18445 = IHEM 3717^{MT}	USA, California, Los Angeles County, soil from gopher hole, *R.S. Pore*	AJ877211	LR136806	LR136807
	CBS 308.65 = ATCC 18446 = IHEM 3703^{MT}	USA, California, Los Angeles County, soil from gopher hole, *R.S. Pore*	LR136977	LR136808	LR136809

Table 1 (cont.)

Species	Culture collection numbers[1,2,3]	Provenance	GenBank/ENA/DDBJ accession numbers[4]		
			ITS	*tubb*	*tef1α*
Arthroderma magnisporum	CBS 132551 = FMR 11770^{T}	Antarctica, South Shetland Archipelago, King George Island, Potter Cave, pellet of *Catharacta skua*, 1996, *W.P. Mac Cormack*	LR756523	LR756531	LR756532
Arthroderma melbournense	CBS 145858 = CCF 6162^{T}	Australia, Melbourne, Nunawading, human toenail-communal podiatry nail dust bag from treatment work, 2017, *S. Jennings & S. Hainsworth*	LR756519	LR756527	LR756528
Arthroderma melis	CBS 669.80 = CCM F-514^{T}	Czech Republic, Moravia, burrow of badger (*Meles meles*), 1973, *K. Křivanec*	AJ877216	HF937404	LR136810
Arthroderma multifidum	CBS 419.71 = ATCC 18440 = IHEM 4432 = IMI 094205 = RV 20033^{MT}	UK, hair and soil from rabbit burrow, *C.O. Dawson*	LR136978	KT155559	LR136811
	CBS 420.71 = ATCC 18441 = IMI 094206^{MT}	UK, hair and soil from rabbit burrow, *C.O. Dawson*	MH860194	LR136812	LR136813
Arthroderma oceanitis	CBS 132552 = FMR 11771^{T}	Antarctica, South Shetland Archipelago, King George Island, Three Brothers Hill, dead juvenile of *Oceanites oceanicus*, 2011, *A. Archuvy*	LR756524	LR756533	LR778323
Arthroderma onychocola	CBS 132920 = CCF 4259^{T}	Czech Republic, Prague, human toenail, 2011, *M. Skořepová*	HF937405	HF937401	LR136814
	CCF 4802	Denmark, Copenhagen, human toenail, 2013, *C.V. Nissen*	LN589976	LN589971	LR136815
Arthroderma phaseoliforme	CBS 364.66^{T}	Venezuela, pelt of mountain rat (*Proechimys guyanensis*), *D. Borelli*	LR136979	LR136816	LR136817
Arthroderma quadrifidum	UAMH 2941 = UAMH 3183 = ATCC 22954 = IMI 84307	Unknown, monoascospore isolate, 1961, *C.O. Dawson & J.C. Gentles*	LR136964	LR136774	LR136775
	UAMH 2942 = UAMH 3184 = UAMH 3187 = ATCC 22955 = IMI 84308	Unknown, monoascospore isolate, 1961, *C.O. Dawson & J.C. Gentles*	LR136965	LR136776	LR136777
	CCF 6385	Czech Republic, building in Brandýs nad Labem, fur of *Mus musculus*, 2019, *Š. Moulíková*	**OM568945**	**OM677694**	**OM568830**
	CCF 6439	Czech Republic, stables in Povodí (Cheb), fur of *Mus musculus*, 2019, *Š. Moulíková*	**OM568946**	**OM677695**	**OM568831**
Arthroderma redellii	CBS 134551^{T}	USA, Wisconsin, Atkinson Mine, wing of hibernating bat (*Myotis lucifugus*), 2012, *M.L. Verant & J.M. Lorch*	KM091307	LR136818	LR136819
Arthroderma rodenticum	**CCF 6383^{T}**	Czech Republic, forest near Sedlečko (Karlovy Vary), fur of *Apodemus flavicollis*, 2019, *Š. Moulíková*	**OM568906**	**OM677657**	**OM568792**
	CCF 6384	Czech Republic, forest near Sedlečko (Karlovy Vary), fur of *Myodes glareolus*, 2019, *Š. Moulíková*	**OM568907**	**OM677658**	**OM568793**
	CCF 6490	Czech Republic, forest near Sedlečko (Karlovy Vary), fur of *Apodemus flavicollis*, 2019, *Š. Moulíková*	**OM568908**	**OM677659**	**OM568794**
	CCF 6491	Czech Republic, forest near Sedlečko (Karlovy Vary), fur of *Apodemus flavicollis*, 2019, *Š. Moulíková*	**OM568909**	**OM677660**	**OM568795**
	CCF 6492	Czech Republic, forest near Sedlečko (Karlovy Vary), fur of *Myodes glareolus*, 2019, *Š. Moulíková*	**OM568910**	**OM677661**	**OM568796**
	AFS1-4B	Czech Republic, forest near Sedlečko (Karlovy Vary), fur of *Apodemus flavicollis*, 2019, *Š. Moulíková*	**OM568911**	**OM677662**	**OM568797**
	AFS2-3	Czech Republic, forest near Sedlečko (Karlovy Vary), fur of *Apodemus flavicollis*, 2019, *Š. Moulíková*	**OM568912**	**OM677663**	**OM568798**
	AFS7-1	Czech Republic, forest near Sedlečko (Karlovy Vary), fur of *Apodemus flavicollis*, 2019, *Š. Moulíková*	**OM568913**	**OM677664**	**OM568799**
	AFS8-1	Czech Republic, forest near Sedlečko (Karlovy Vary), fur of *Apodemus flavicollis*, 2019, *Š. Moulíková*	**OM568914**	**OM677665**	**OM568800**
	AFS12-3	Czech Republic, forest near Sedlečko (Karlovy Vary), fur of *Apodemus flavicollis*, 2019, *Š. Moulíková*	**OM568915**	**OM677666**	**OM568801**
	AFS15-3	Czech Republic, forest near Sedlečko (Karlovy Vary), fur of *Apodemus flavicollis*, 2019, *Š. Moulíková*	**OM568916**	**OM677667**	**OM568802**
	CGS1-3	Czech Republic, forest near Sedlečko (Karlovy Vary), fur of *Myodes glareolus*, 2019, *Š. Moulíková*	**OM568917**	**OM677668**	**OM568803**
	CGS2-4	Czech Republic, forest near Sedlečko (Karlovy Vary), fur of *Myodes glareolus*, 2019, *Š. Moulíková*	**OM568918**	**OM677669**	**OM568804**
	CGS5-1	Czech Republic, forest near Sedlečko (Karlovy Vary), fur of *Myodes glareolus*, 2019, *Š. Moulíková*	**OM568919**	**OM677670**	**OM568805**
	CGS6-3	Czech Republic, forest near Sedlečko (Karlovy Vary), fur of *Myodes glareolus*, 2019, *Š. Moulíková*	**OM568920**	**OM677671**	**OM568806**
	CGS8-7	Czech Republic, forest near Sedlečko (Karlovy Vary), fur of *Myodes glareolus*, 2019, *Š. Moulíková*	**OM568921**	**OM677672**	**OM568807**
	CGS9-1	Czech Republic, forest near Sedlečko (Karlovy Vary), fur of *Myodes glareolus*, 2019, *Š. Moulíková*	**OM568922**	**OM677673**	**OM568808**
Arthroderma silverae	CBS 141576 = UAMH 6517^{T}	Norway, Svalbard, Glundnest area, Ny-Ålesund, dung of Arctic fox (*Alopex lagopus*), 1988, *R. Currah*	LR136980	LR136820	LR136821
Arthroderma simile	**CCF 6387^{T}**	Czech Republic, forest near Sedlečko (Karlovy Vary), fur of *Myodes glareolus*, 2019, *Š. Moulíková*	**OM568896**	**OM677646**	**OM568781**
	CCF 6281 = 07MA15	USA, Massachusetts, soil from bat hibernaculum, 2008/2009, *J.M. Lorch*	**OM568897**	**OM677647**	**OM568782**
Arthroderma terrestre	UAMH 657 = CCF 6419^{T}	Australia, soil, *E.B. Durie*	LR756521	LR756534	LR756535
	UAMH 662	Unknown locality, soil, 1959	LR756522	LR756536	LR756537
Arthroderma thuringiense	CBS 417.71 = ATCC 22648 = IMI 134993 = UAMH 3431^{T}	Germany, Thüringen, mouse skin, 1964, *H.A. Koch*	AJ877215	HF937402	LR778324
Arthroderma tuberculatum	CBS 473.77 = ATCC 26700 = UAMH 873^{T}	USA, Illinois, Urbana, feather of *Turdus americanis*, 1954, *H.H. Kühn*	LR136981	LR136822	LR136823
	CCF 6170	Australia, Far North Queensland, Cairns, human toenail-communal podiatry nail dust bag from treatment work, 2016, *S. Hainsworth*	LR778320	LR778321	LR778322
	UAMH 2831	India, Puné, soil, 1967, *A.A. Padhye*	**OM568947**	–	**OM568832**

Table 1 (cont.)

Species	Culture collection numbers[1,2,3]	Provenance	GenBank/ENA/DDBJ accession numbers[4]		
			ITS	*tubb*	*tef1α*
Arthroderma uncinatum	CBS 315.65^{MT}	USA, California, Kern County, soil, 1962, *O.A. Plunkett*	MH858587	LR136824	LR136825
	CBS 316.65^{MT}	USA, California, Kern County, soil, 1962, *O.A. Plunkett*	MH858588	LR136826	LR136827
Arthroderma vespertilii	CBS 355.93 = FMR 3752 = IMI 357403 = RV 27093^{T}	Zaire, cave near Kibisi, intestinal content of the bat, 1971, *C. de Vroey*	AJ007846	LR136828	LR136829
Arthroderma psychrophilum	CCF 5960 = NWHC 44738-022_I3^{T}	USA, Wisconsin, Grant County, wing skin of hibernating *Myotis lucifugus*, 2013, coll. *J.P. White*, isol. *J.M. Lorch*	**OM568901**	**OM677652**	**OM568787**
	CCF 5856 = CCF 6136	Czech Republic, Bohemian Karst, air in an underground tunnel of Velká Amerika, 2014, *A. Kubátová*	**OM568902**	**OM677653**	**OM568788**
	CCF 6422	Czech Republic, farm in Hartoušov (Cheb), fur of *Mus musculus*, 2019, *Š. Moulíková*	**OM568903**	**OM677654**	**OM568789**
	CCF 6423	Czech Republic, farm in Loužek (Cheb), fur of *Mus musculus*, 2019, *Š. Moulíková*	**OM568904**	**OM677655**	**OM568790**
	CCF 6424	Czech Republic, farm in Hartoušov (Cheb), fur of *Mus musculus*, 2019, *Š. Moulíková*	**OM568905**	**OM677656**	**OM568791**
Arthroderma zoogenum	**CCF 6382^{T}**	Czech Republic, forest near Sedlečko (Karlovy Vary), fur of *Myodes glareolus*, 2019, *Š. Moulíková*	**OM568898**	**OM677648**	**OM568783**
	CCF 5959 = NWHC 44736-13-C4-I1	USA, Massachusetts, skin of *Crotalus horridus*, 2013, coll. *J. Condon*, isol. *J.M. Lorch*	**OM568899**	**OM677649**	**OM568784**
	VMZ Sob1.1-19	Russia, skin lesions in wild *Martes zibellina*, 2019, *R.S. Ovchinnikov*	**OM568900**	**OM677650**	**OM568785**
	IFM 41172	Finland, *Meles meles* (badger), 1990, *R. Aho*	AB458161	**OM677651**	**OM568786**
Pectinotrichum llanense (outgroup)	CBS 882.71 = ATCC 18921 = IHEM 4440 = IMI 155643 = RV 22834^{T}	Venezuela, savanna soil, *G.F. Orr*	LR136983	LR136832	LR136833

[1] Culture collection acronyms: ATCC, American Type Culture Collection, Manassas, Virginia, USA; IHEM (BCCM/IHEM), Belgian Coordinated Collections of Microorganisms, Fungi Collection: Human and Animal Health, Sciensano, Brussels, Belgium; CBS, Westerdijk Fungal Biodiversity Institute (formerly Centraalbureau voor Schimmelcultures), Utrecht, Netherlands; CCF, Culture Collection of Fungi, Prague, Charles University, Department of Botany, Czech Republic; CCM (F-), Czech Collection of Microorganisms, Brno, Czech Republic; CDC, Centers for Disease Control, Atlanta, Georgia, USA; DSM, Leibniz Institute DSMZ-German Collection of Microorganisms and Cell Cultures, Braunschweig, Germany; FMR, Faculty of Medicine, Reus, Spain; IFM, Culture Collections for Pathogenic Fungi and Actinomycetes, Medical Mycology Research Center, Chiba University, Chiba, Japan; IMI, CABI's collection of fungi and bacteria, Wallingford, UK; NHL, National Institute of Hygienic Sciences, Tokyo, Japan; NRRL, Agricultural Research Service Culture Collection, Peoria, Illinois, USA; NWHC, identifier of National Wildlife Health Center, Madison, Wisconsin, USA; RV, former collection of Raymond Vanbreuseghem (now incorporated in BCCM/IHEM); UAMH, UAMH Centre for Global Microfungal Biodiversity (formerly University of Alberta Microfungus collection and Herbarium), Gage Research Institute, University of Toronto, Toronto, Canada. Other acronyms represent personal strain numbers (without permanent preservation).

[2] Ex-type strains are designated by a superscript 'T'; in case that the dried type specimen included two opposite mating type strains, these strains are designated 'MT' (mating type); authentic strains are designated by superscript 'AUT'.

[3] Collection numbers in **bold** were isolated in this study from wild rodents.

[4] Accession numbers in **bold** were generated in this study.

models: K80+I+G substitution model was proposed for the *tubb* introns; HKY+G model for *tef1α* introns; TrNef+I+G model for *tubb* and *tef1α* exons; TrNef+G model for the ITS1 region; K80+I+G model for the 5.8S region; and TrNef+I+G model for the ITS2 region. The ML tree was constructed with IQ-TREE v. 1.4.4 with nodal support determined by non-parametric bootstrapping (BS) with 1 000 replicates (Nguyen et al. 2015). *Pectinotrichum llanense* CBS 882.71 was used as outgroup.

Bayesian posterior probabilities (PP) were calculated using MrBayes v. 3.2.6 (Ronquist et al. 2012). The optimal partitioning scheme and substitution models were selected as described above. The optimal partitioning scheme divided the dataset into five partitions with the following substitution models: K80+I+G substitution model was proposed for the *tubb* introns; HKY+G model for *tef1α* introns; SYM+I+G model for *tubb* and *tef1α* exons; SIM+I+G for the ITS1 and ITS2 regions; and K80+I+G for the 5.8S region. The analysis ran for 10^7 generations; two parallel runs with four chains each were used, every 1000th tree was retained, and the first 25 % of trees were discarded as burn-in. Convergence was assessed by examining the likelihood plots in Tracer v. 1.7 (Rambaut et al. 2018).

Phenotypic studies

Macromorphological characters of colonies were observed on SDA, MEA, potato dextrose agar (PDA; HiMedia, Mumbai, India) and oatmeal agar (OA; HiMedia, Mumbai, India). Petri dishes were inoculated using three-point inoculation and incubated at 25 °C in darkness. Colour codes and names followed the conventions described by Kornerup & Wanscher (1978). Growth at 30 and 37 °C was tested on MEA plates. Colonies were observed and photographed using a Canon EOS 500D. Preparations for light microscopy were made from material harvested from 14-d-old cultures on MEA plates and stained with lactic acid with cotton blue. Microphotographs were taken with an Olympus BX51 microscope and Olympus DP72 camera. Micromorphological characters were measured using QuickPHOTO MICRO v. 3.0 (PROMICRA, Prague, Czech Republic).

For the purposes of comparing closely related species, the following isolates were also examined: *A. cuniculi*: CBS 492.71, CBS 495.71; *A. insingulare*: CBS 521.71, CBS 522.71, UAMH 754, UAMH 2922, UAMH 2923, UAMH 2925, UAMH 3439, UAMH 3440; *A. phaseoliforme*: CBS 364.66; *A. tuberculatum*: CBS 473.77.

Induction of sexual morph

Induction of the sexual morph for some of the heterothallic species was done on *Guizotia abyssinica* agar (GAA) (De Vroey 1964, Symoens et al. 2013). Isolates of different mating-type gene idiomorphs were inoculated on the same plate approximately 10 mm apart. Inoculated plates were incubated at 17 °C for 7 wk and were checked once per wk for the presence of ascomata.

Statistical analysis

Micromorphological data were statistically analysed in R v. 3.6.3 (R Core Team 2020) using ANOVA and Tukey's HSD test. The curves of individual rarefaction of species richness (Krebs 1989) for *Artthroderma* strains isolated in this study were generated in PAST v. 4.03 (Hammer et al. 2001) to estimate expected species richness.

Phylogeny of environmental sequences and biogeography

Principally, we followed the workflow of Réblová et al. (2021a, b). To study *Arthroderma* diversity among environmental sequences, the full-length ITS1+5.8S and ITS2 sequences of all *Arthroderma* species from Hainsworth et al. (2021) (hereafter referred to as the 'reference dataset') were searched against

the GlobalFungi Database release 3 (data from 36 684 samples, 367 studies and 582 264 149 ITS1 and 526 638 147 ITS2 sequences; the list of studies queried is provided in Table S1) using the BLAST algorithm. For each sequence, the first 500 top matches, representing haplotypes with 85–100 % sequence similarity, were downloaded and the dataset was dereplicated (i.e., identical sequences were removed) (Table S2). The sequences ascribable to *Arthroderma* deposited in the NCBI GenBank database were obtained using a BLASTn search (25 July 2021) of ITS sequences from the reference dataset and downloading sequences with similarity ≥ 85 % (hereafter referred to as the 'NCBI GenBank dataset'). This selection contained sequences of *Arthroderma* and related genera. Finally, two datasets were assembled consisting of either 1) full length ITS1; or 2) ITS2 metabarcoding data, each supplemented with the full length ITS reference and NCBI GenBank datasets together with outgroup sequences. The datasets were aligned using MAFFT v. 7 (Katoh et al. 2019), and *Arthroderma* genus boundaries were inferred from ML trees computed in Phyml v. 3.1 (Guindon et al. 2009) using the GTR model and SH-based –aLRT statistics for branch support statistics. The datasets were pruned by removing sequences not within the genus *Arthroderma*, and most of the singletons (i.e., haplotypes represented in the database by a single read) from metabarcoding data were also removed. The only metabarcoding singletons retained were those that clustered with the newly described species. The sequence manipulations were done in SEED2 (Větrovský et al. 2018). In the final ML trees, the phylotypes were defined as terminal, well supported clades containing strains of single species or having similar genetic similarity. For known species, genetic variation within clades ranged from 97 % (*A. crocatum*) to 98–100 % (others) (Table S1), and we therefore used a sequence similarity of 98 % for defining phylotypes consisting entirely of metabarcoding data. For each phylotype, data about occurrence across environmental samples and metadata (location, substrate, biome, climatic data, pH) were recorded (Table S1).

RESULTS

Phylogeny

Of the 63 rodents sampled, we obtained 29 *Arthroderma* strains (Table 1). Based on our culture results, the prevalence of *Arthroderma* in captured rodents were 15 % (5/33) in house mice, 56 % (9/16) in yellow-necked mice, and 71 % (10/14) in bank voles (Table 2).

The study was further supplemented with genetically related strains representing identical or sister species to those obtained from rodents to acquire a more robust phylogeny and to strengthen taxonomic conclusions. For the phylogenetic analysis, the final alignment contained 94 combined ITS, *tubb*, and *tef1-α* sequences with 1 880 positions of which 988 were variable and 798 were parsimony informative.

The topology of the Bayesian tree (Fig. 1) was nearly identical to the best scoring ML tree. The phylogeny supported the recognition of all 27 *Arthroderma* species previously accepted by Hainsworth et al. (2021) and revealed an additional four well-supported clades corresponding to the four newly described species in this study: *A. rodenticum*, *A. zoogenum*, *A. simile*, and *A. psychrophilum* (see section Taxonomy).

These newly proposed species were resolved in three different clades/species complexes *sensu* Hainsworth et al. (2021):

– The *A. uncinatum* clade encompassed *A. rodenticum* and *A. simile* spp. nov. In phylogenetic trees, *A. rodenticum* formed a well-supported subclade with *A. insingulare* (Bayesian PP of 0.95 and an ML BS of 90 %). *Arthroderma simile* sp. nov. was sister to this subclade. All three species together formed a clade sister to the clade consisting of *A. gloriae*, *A. gertleri*, *A. lenticulare*, and *A. uncinatum.*

– The *A. silverae* clade was composed of three species, including *A. psychrophilum* sp. nov. In our analysis, the clade gained full statistical support. *Arthroderma psychrophilum* was placed sister to the subclade formed by *A. silverae* and *A. oceanitis*.

– The *A. tuberculatum* clade encompassed four species including *A. zoogenum* sp. nov., *A. cuniculi*, *A. tuberculatum*, and *A. phaseoliforme*. *Arthroderma zoogenum* clustered with *A. cuniculi* with high support (0.98 / 97 %).

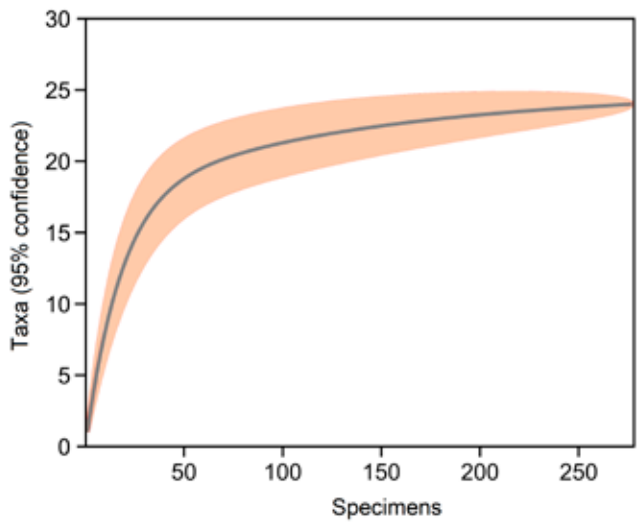

Fig. 2 Individual rarefraction curve (with 95-percent confidence intervals) for *Arthroderma* species occurring on the hair of all rodent individuals sampled in the study. The curve shows dependence of the increasing estimated number of new taxa on increasing sampling effort. The estimated number of new taxa expected to be isolated from the same material using the same approach but with a larger sample size. Around 25 species of *Arthroderma* are predicted when collecting more than 250 *Arthroderma* isolates using the same methodology. This indicates that the number of *Arthroderma* species were likely not saturated by sampling in this study.

Table 2 Prevalence and diversity of *Arthroderma* in captured individuals of three rodent species.

	Captured individuals	Number and prevalence (%) of *Arthroderma* positive individuals	Number of *Arthroderma* strains	*Arthroderma* species
house mouse	33	5 (15 %)	5	*A. psychrophilum* sp. nov., *A. quadrifidum*
yellow-necked mouse	16	9 (56 %)	9	*A. rodenticum* sp. nov.
bank vole	14	10 (71 %)	15	*A. rodenticum* sp. nov., *A. zoogenum* sp. nov., *A. simile* sp. nov., *A. curreyi*, *A. cuniculi*, *A. crocatum*
Total	63	24 (38 %)	29	

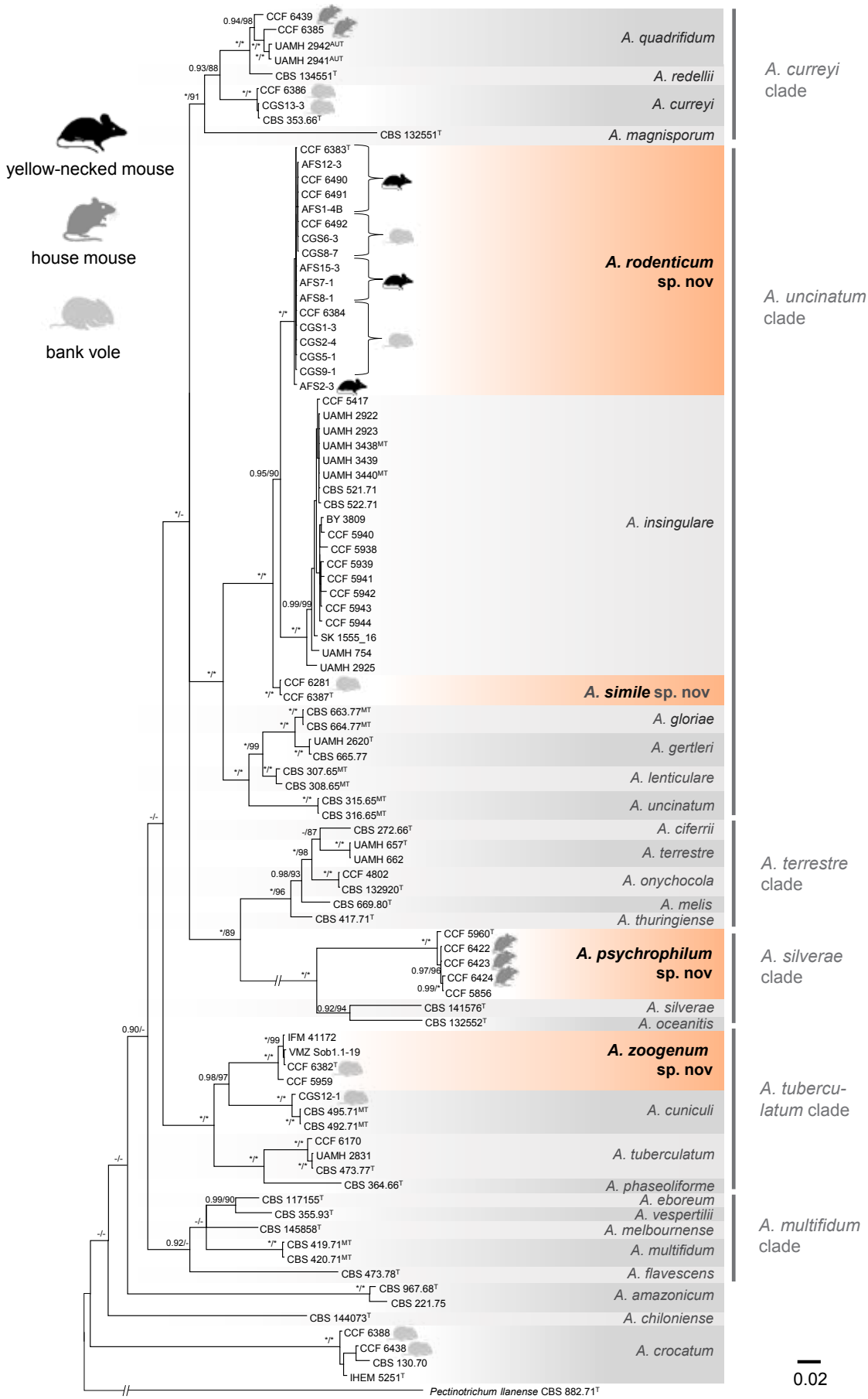

Fig. 1 Phylogenetic relationships of *Arthroderma* species inferred from maximum likelihood analysis of the combined, 3-gene data set: ITS region of the rDNA, β-tubulin (*tubb*) gene and translation elongation factor 1-α (*tef1α*) gene. Bayesian posterior probability (PP) and maximum likelihood bootstrap support (BS) values are appended to nodes; only PP ≥ 0.90 and BS ≥ 70 % are shown, whereas asterisks indicate full support (1.00 PP or 100 % BS); lower supports are indicated with a hyphen; ex-type strains are designated by a superscript 'T', in instances where the dried type specimen included two opposite mating type strains, these strains are designated 'MT' (mating type), authentic strains are designated by superscript 'AUT'. The tree is rooted with *Pectinotrichum llanense* CBS 882.71.

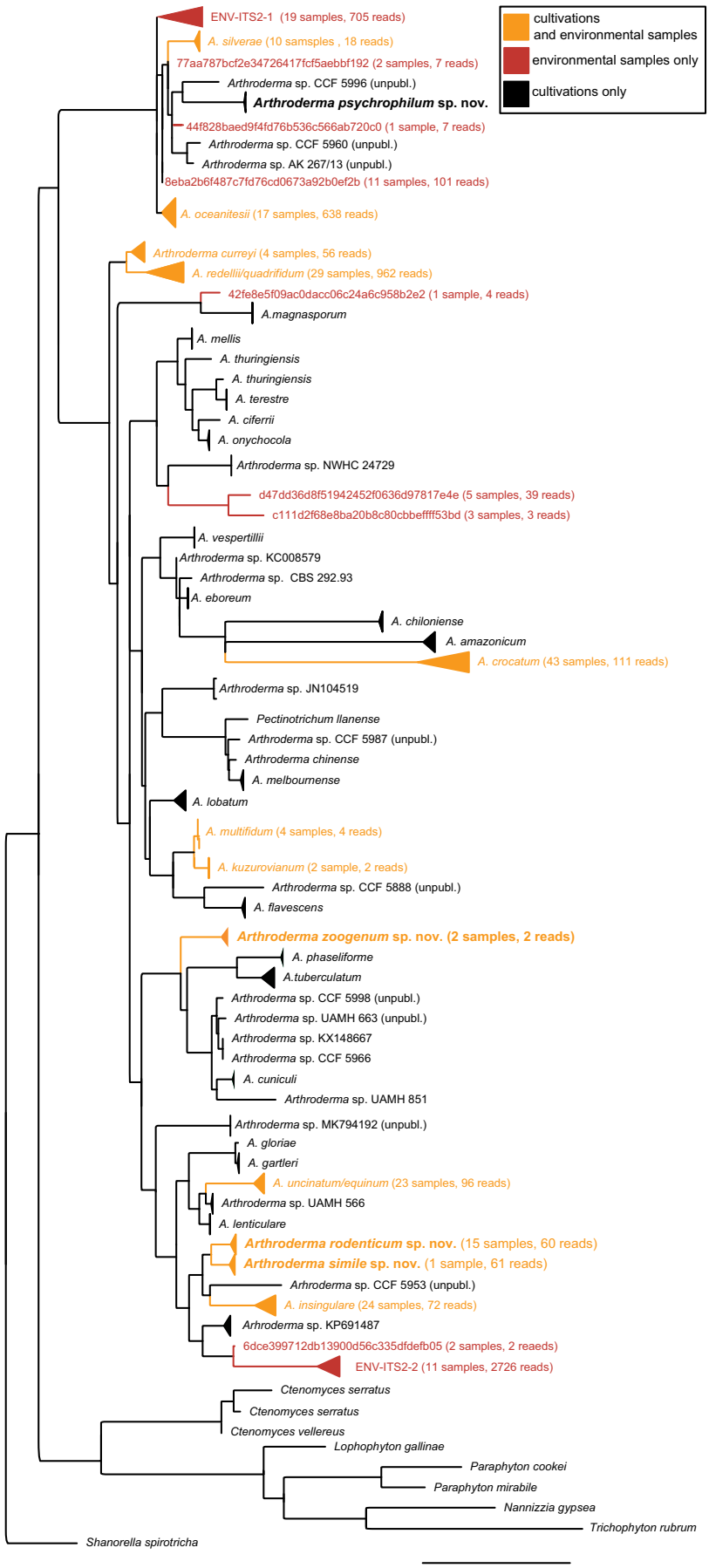

Fig. 3 Phylogenetic relationships among *Arthroderma* strains based on data from NCBI GenBank and the GlobalFungi Database. Data from the GlobalFungi Database include only non-singleton ITS2 sequences (i.e., those presented in the database with at least two reads). The titles of environmental sequences contain the sequence and sample codes taken from the GlobalFungi Database. Terminal clades have been collapsed using FigTree v. 1.4.4 (Rambaut 2020). The tree was rooted with *Shanorella spirotricha*, its branch is shown as one-quarter of the actual length. Phylotypes are differentiated by colours: those obtained from culture-dependent methods are shown in black, those detected by culture-independent methods are shown in red, and those detected by both methodologies are displayed in orange.

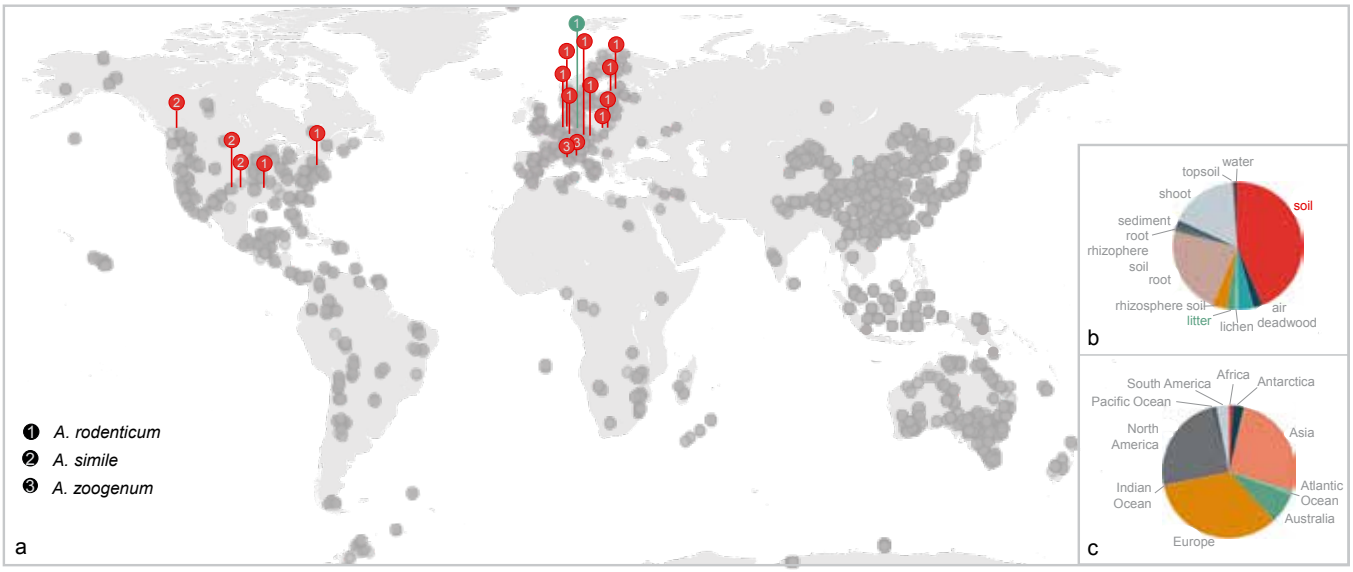

Fig. 4 Geographical distribution and substrate affinity of newly described *Arthroderma* species based on the ITS1 and ITS2 data from the GlobalFungi Database. See Table S1 for primary data. a. New taxa described herein are represented as large circles with unique numbers (1–3) and are coloured according to the substrate in which they were detected (as indicated in (b)). Locations represented in the GlobalFungi Database for which the new taxa were not detected are shown as grey dots. The uneven representation of individual habitats and sites in the GlobalFungi database is demonstrated by the following graphs: b. pie chart displaying the substrates/habitats sampled for the various datasets in the GlobalFungi Database and c. the geographic locations of all sample sets deposited in the GlobalFungi Database.

Arthroderma species diversity in rodents

Considerable *Arthroderma* species richness was found in all three rodent host species sampled. The highest *Arthroderma* species richness (n = 6) was observed in bank voles (n = 14) from a single locality near Karlovy Vary in Czech Republic. These were identified as three new (*A. rodenticum*, *A. zoogenum*, and *A. simile*) and three previously described species (*A. curreyi*, *A. cuniculi*, and *A. crocatum*). Some individual voles were carriers of more than one *Arthroderma* species. All individual bank voles were from the same locality as 16 yellow-necked mice. However, the yellow-necked mice from this location hosted only one *Arthroderma* species, *A. rodenticum*. The lowest *Arthroderma* species richness occurred in house mice (n = 33) sampled from three localities in the Czech Republic; these mice hosted only two *Arthroderma* species: *A. psychrophilum* sp. nov. and *A. quadrifidum* (Table 2). To demonstrate the species diversity in the various rodent hosts, the cumulative species count against number of studied *Arthroderma* strains isolated from all rodent species was plotted (Fig. 2). The individual rarefaction curve showed that we did not capture the likely diversity of *Arthroderma* present at our study sites. Specifically, we recovered eight taxa, well below the 25 *Arthroderma* species predicted to occur at the sites (Fig. 2).

Environmental data mining

The data from massive parallel sequencing technologies showed poor presence of *Arthroderma* in screened environmental samples (bulk soil, roots, plant shoots, and deadwood). From the environmental, non-singleton sequences, 5057 reads in the ITS2 (0.001 % of all sequences) and 65 (0.0001 % of all sequences) in the ITS1 dataset could be ascribed to *Arthroderma* (Fig. 3, Appendix 2).

For the ITS2 dataset (Fig. 3), phylotypes corresponded to clades of sequences with a similarity ≥ 97 % (*A. crocatum*), ≥ 98 % (*A. quadrifidum*/*A. redellii* and *A. insingulare*) or ≥ 98.8 % (others). Out of the total number of 63 ITS2 phylotypes, 41 (i.e., 65 %) were found by cultivation-based studies only (Fig. 3, black), 12 by both cultivation dependent and independent studies (Fig. 3, orange), and nine originated from environmental samples only (Fig. 3, red). Only four phylotypes exclusively found in environmental samples could be considered common (Fig. 3, Table S2). Inside the *A. silverae*/*A. oceanitis* clade, the phylotype ENV-ITS2-1 consisted of a rather heterogeneous set of haplotypes (similarity > 98.8 % in ITS2) from South America, Europe, and Asia. The second one, ENV-ITS2-9, belonged to the *A. insingulare* clade and was abundant in numerous soil samples across Australia. Phylotype ENV-ITS2-4 (*A. silverae*/*A. oceanitis* clade) was found in Antarctica, and ENV-ITS2-6 (close to *Arthroderma* sp. NWHC 24729) was found in Australia and South America. The other less abundant phylotypes were found in Europe (ENV-ITS2-2), Antarctica (ENV-ITS2-5), Australia (ENV-ITS2-7), and North America (ENV-ITS2-8) (Table S1). Of the 48 clades represented in the ITS1 dataset (Appendix 2), five were found by both culture-dependent and culture-independent approaches, and these clades overlapped with those found in the ITS2 dataset (*A. curreyi*, *A. quadrifidum*/*A. redellii*, *A. silverae*, *A. crocatum*, *A. uncinatum*). The rest of the phylotypes were represented by environmental DNA detections only.

Concerning geographical distribution, some of the phylotypes were globally distributed (*A. crocatum*, *A. quadrifidum*, *A. uncinatum*). The *A. insingulare* phylotype was found in Europe, North America, Australia, and Antarctica, and the *A. oceanitis* phylotype was found in Europe, East Asia, and Antarctica (Table S1). Others appeared to be more restricted in their geographic distributions, being detected only in Europe (*A. curreyi*, *A. multifidum*), Eurasia (*A. silverae*), or the Northern Hemisphere (*Chrysosporium keratinophilum*, *A. uncinatum*).

The biogeography of the new species was evaluated in more detail using data mining of both ITS1 and ITS2 data (Fig. 4, Table S1). Three of the four newly described species were found in environmental samples generated by next-generation sequencing (*A. simile*, *A. zoogenum*, and *A. rodenticum*) from Central and Northern Europe or North America (Fig. 4, Table S1; see Taxonomy for detailed data). All environmental sampling locations were in forest, grassland, or tundra habitats with relatively cold climates (mean annual temperature 0–7.8 °C).

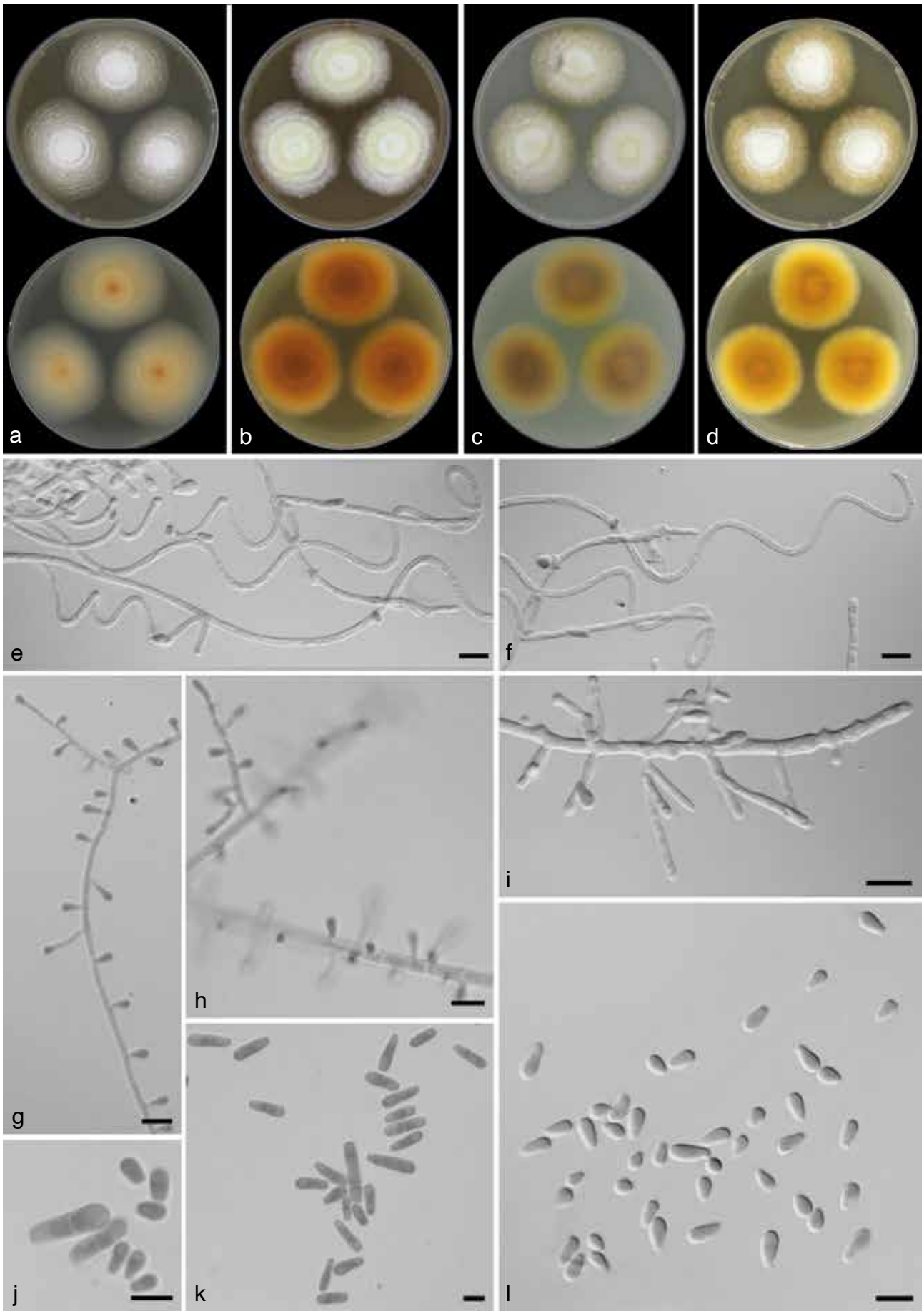

Fig. 5 Asexual morph of *Arthroderma rodenticum* sp. nov. a–b. Colonies after 2 wk at 25 °C on malt extract agar (a), Sabouraud's dextrose agar (b), oatmeal agar (c) and potato dextrose agar (d); e–f. spiral hyphae; g–i. sparsely branched conidiophores; j. microconidia and macroconidia; k. smooth-walled, cigar-shaped to cylindrical macroconidia with two to three cells; l. smooth-walled, clavate microconidia. — Scale bars: 10 µm.

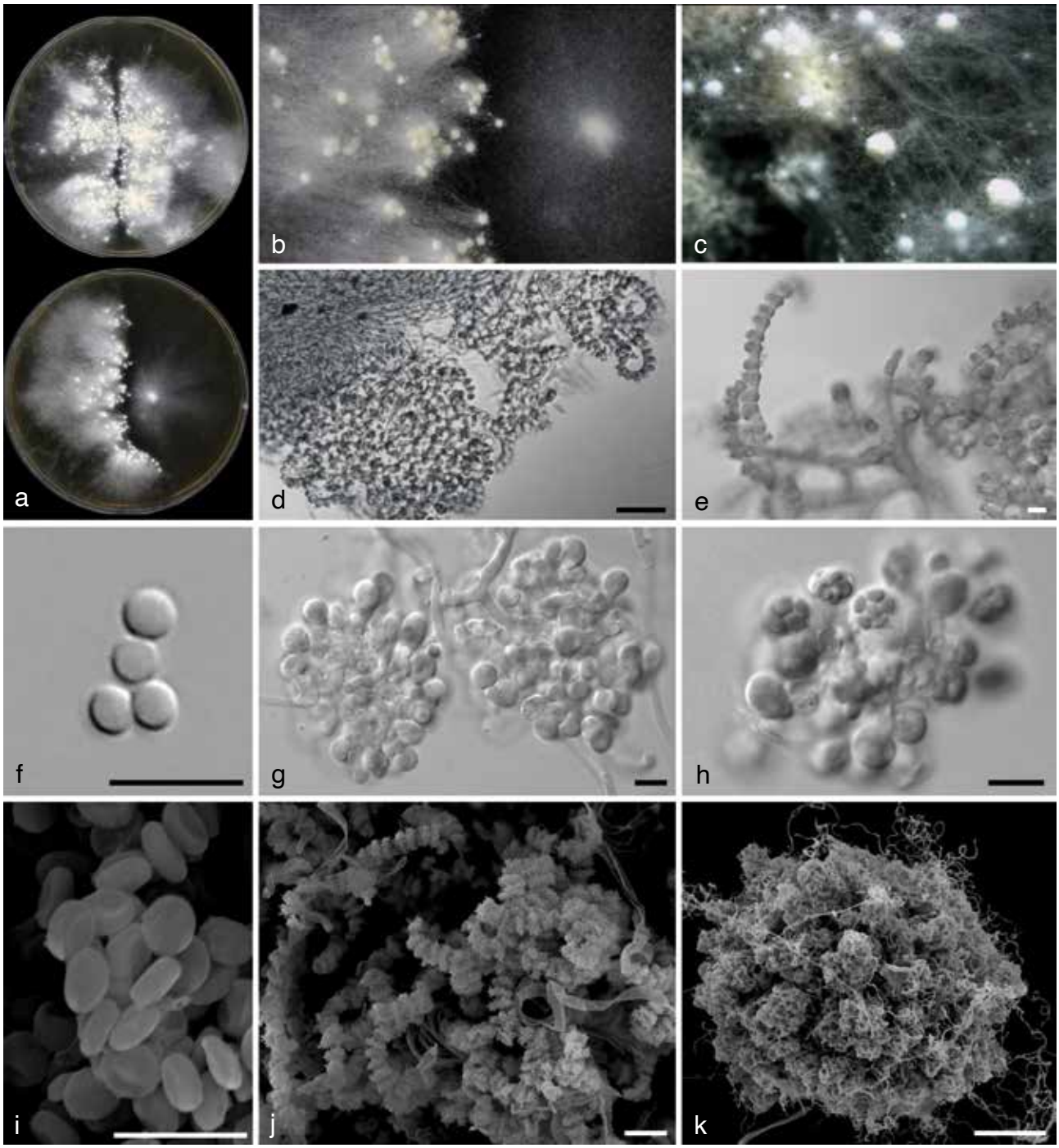

Fig. 6 Sexual morph of *Arthroderma rodenticum* sp. nov. a. Crossed strains after 6 wk at 17 °C on *Guizotia abyssinica* agar (upper subfigure: isolates AFS8-1 × CCF 6383, lower subfigure: isolates AFS8-1 × CGS2-4); b–c. detail of ascomata; d–e. echinulate peridial hyphae, dumbbell-shaped peridial cells with distinct constrictions; f. smooth-walled, oval ascospores; g–h. asci; i–k. scanning electron microscopy (SEM) photographs of ascospores (i), peridial hyphae (j) and ascoma (k). — Scale bars: d = 50 µm, e–h, j = 10 µm, i = 5 µm, k = 100 µm.

TAXONOMY

Arthroderma rodenticum Moulikova, Kubátová & Cmokova, *sp. nov.* — MycoBank MB 845979; Fig. 5, 6

Etymology. Latin, *rodenticus -a -um*, referring to the high prevalence in rodents.

Typus. Czech Republic, forest near Sedlečko, Karlovy Vary region, fur of *Apodemus flavicollis*, 2019, *Š. Moulíková* (holotype PRM 954603, culture ex-type CCF 6383 = AFS11-3, mating-type gene idiomorph MAT1-2-1).

Vegetative mycelium consists of hyaline, smooth-walled, septate hyphae; spiral hyphae not observed on vegetative mycelium, only rarely in association with peridial hyphae. *Conidiophores* simple, conidiogenous hyphae unbranched or laterally branched max. two times. *Microconidia* hyaline, smooth-walled, non-septate, clavate, 2–11.5 (4.8 ± 1.3) × 1.5–4 (2.3 ± 0.4) µm. *Macroconidia* hyaline, smooth-walled, septate with two to four cells, cigar-shaped to cylindrical, 6.5–29.5 (11.3 ± 3.4) × 2–4.5 (3.1 ± 0.4) µm. *Pseudoascomata* consisting of clusters of conidiophores, peridial hyphae and occasionally spiral hyphae. *Peridial hyphae* hyaline, hooked; *peridial cells* dumbbell-shaped, finely echinulate compared to coarsely echinulate peridial hyphae on true ascomata. Heterothallic species. *Ascomata* produced on GAA medium, 300–600 µm diam; *peridial hyphae* hyaline, hooked; *peridial cells* dumbbell-shaped, coarsely echinulate with distinct constrictions, 6.5–13 (9.1 ± 1.3) µm long with 3–7 (5 ± 0.8) µm diam at the enlarged ends and 2–5.5 (3.2 ± 0.5) µm diam at constrictions. *Asci* ovate to globose, 4.5–6.5 (5.3 ± 0.4) × 3–5.5 (4.3 ± 0.4) µm; *ascospores* hyaline, smooth-walled, non-septate, oval, 2–3 (2.3 ± 0.2) × 1–2.5 (1.7 ± 0.2) µm.

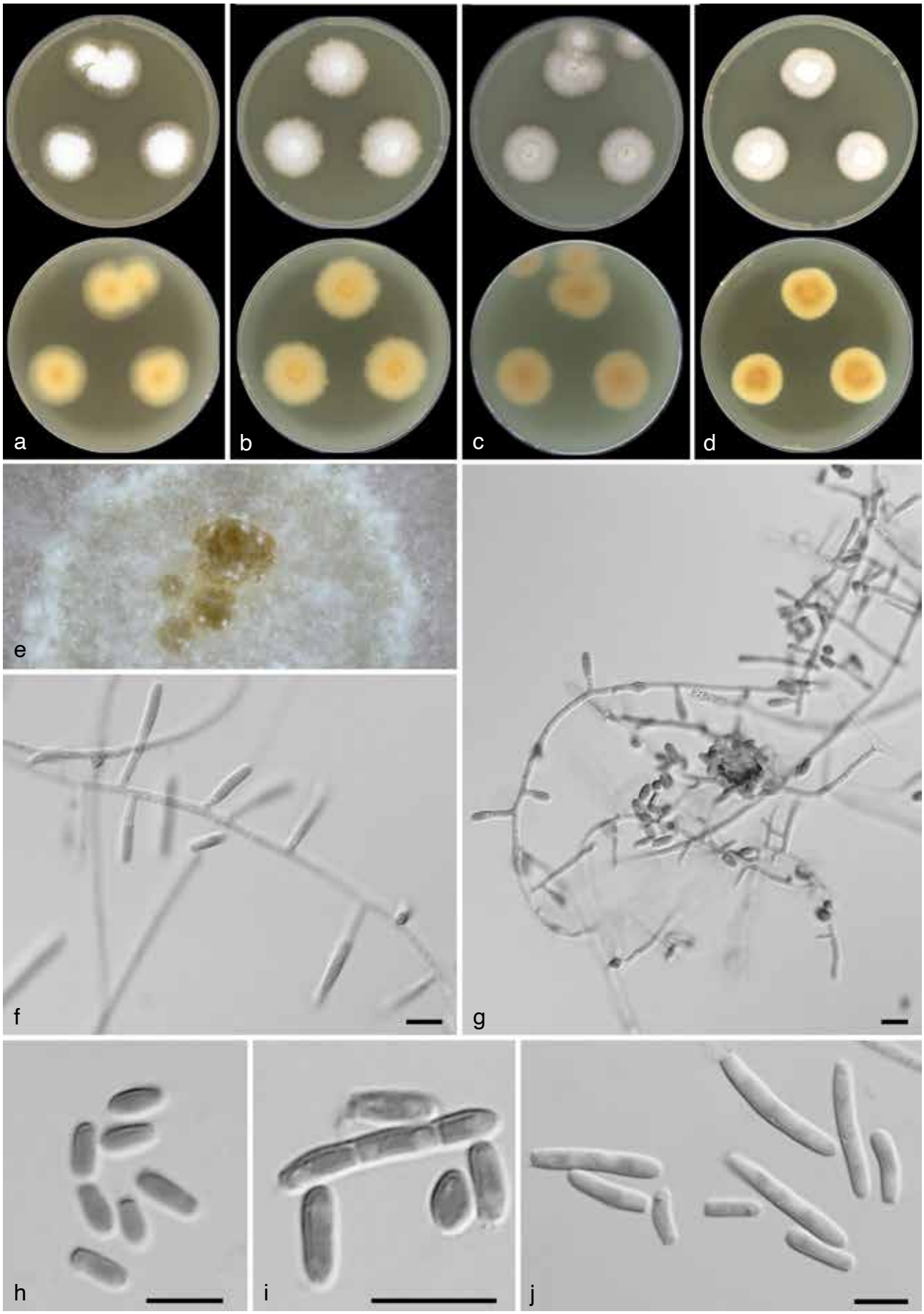

Fig. 7 *Arthroderma simile* sp. nov. a–b. Colonies after 2 wk at 25 °C on malt extract agar (a), Sabouraud's dextrose agar (b), oatmeal agar (c), and potato dextrose agar (d); e. detail of colony with exudate on oatmeal agar; f–g. sparsely branched conidiophores; h. smooth-walled, cylindrical to clavate microconidia; i. smooth-walled, cylindrical to clavate microconidia and smooth-walled, cylindrical macroconidia consisting of three cells; j. smooth-walled, cylindrical macroconidia consisting of two to four cells. — Scale bars: 10 µm.

Culture characteristics (after 14 d) — Colonies on MEA at 25 °C 36–47 mm diam, velvety to granular, centrally raised with filamentous margins, white to yellowish white (3A2), reverse yellowish white (3A2) with yellowish orange centre (4B8). Colonies on SDA at 25 °C 30–47 mm diam, velvety to granular, centrally raised with concentric pattern, white to light yellow (1A6, 2A5), reverse yellow (2A7) with brown centre (6D7). Colonies on OA at 25 °C 28–43 mm diam, floccose to velvety, centrally raised with filamentous margins, white to yellowish white (3A2), reverse yellow (3A6) with yellowish brown centre (5E6). Colonies on PDA at 25 °C 25–41 mm diam, velvety to cottony, centrally raised with concentric pattern, white to pastel yellow (1A8, 2A4), reverse yellow (2A6) with brown centre (6E5). Colonies on MEA at 30 °C 14–24 mm diam, colony centre raised and velvety, surrounded by filamentous mycelium, concentric pattern, white to sulphur yellow (1A5, 2A4), reverse yellowish white with light yellow to yellowish brown centre (3A5, 5E7). No growth on MEA at 37 °C.

Ecology — The prevalence of *A. rodenticum* in the examined rodents was very high: ~64 % (9/14) in bank voles and 50 % (8/16) in yellow-necked mice. Besides rodents, the species was also reported from human clinical material in Switzerland (isolate bM 128, ITS sequence accession JX122382) (De Respinis et al. 2013). Based on metabarcoding data, the species is rather common in temperate Europe: Czech Republic (Baldrian et al. 2016, Mašínová et al. 2017), Denmark (Frøslev et al. 2019), Estonia (Oja et al. 2017, Bahram et al. 2020), Hungary (Geml 2019), Germany (Purahong et al. 2018) and Poland (Prada-Salcedo et al. 2021). It was also detected in the forest soil in Kansas and Massachusetts (Anthony et al. 2017). The environmental samples originated mostly from soil, rarely from deadwood or litter collected in forest or shrubland habitats with mean annual temperatures ranging from 7 to 12 °C (average 7.9 °C) (Table S1, Fig. 4).

Additional isolates examined. Czech Republic, forest near Sedlečko, Karlovy Vary region, fur of *Apodemus flavicollis*, 2019, *Š. Moulíková* (CCF 6490 = AFS13T-2), MAT1-1-1; ibid. (CCF 6491 = AFS16-1ZN), MAT1-2-1; ibid. (AFS1-4B), MAT1-1-1; ibid. (AFS2-3), MAT1-1-1; ibid. (AFS7-1), MAT1-2-1; ibid. (AFS8-1), MAT1-1-1; ibid. (AFS12-3), MAT1-2-1; ibid. (AFS15-3), MAT1-2-1; forest near Sedlečko, Karlovy Vary region, fur of *Myodes glareolus*, 2019, *Š. Moulíková* (PRM 954604, CCF 6492 = CGS14-2), MAT1-1-1; ibid. (CCF 6384 = CGS13-1), MAT1-2-1; ibid. (CGS1-3), MAT1-2-1; ibid. (CGS2-4), MAT1-2-1; ibid. (CGS5-1), MAT1-1-1; ibid. (CGS6-3), MAT1-2-1; ibid. (CGS8-7), MAT1-1-1; ibid. (CGS9-1), MAT1-1-1.

Notes — *Arthroderma rodenticum* can be differentiated from closely related species, *A. insingulare* and *A. simile*, by concentric pattern of colonies on MEA, SDA and PDA. *Arthroderma rodenticum* and *A. insingulare* (MEA: 31–40 mm, SDA: 32–40 mm, OA: 28–37 mm, PDA: 29–36 mm) grow faster at 25 °C on all cultivation media compared to *A. simile*, which is also unable to grow at 30 °C in contrast to the first two mentioned species. *Arthroderma rodenticum* produces statistically significantly (Tukey's HSD test, $p < 0.05$) shorter and broader micro- and macroconidia compared to *A. simile*.

Arthroderma simile Moulikova, Hubka, J.M. Lorch & Cmokova, *sp. nov.* — MycoBank MB 845980; Fig. 7

Etymology. Latin, *similis -e*, referring to the morphological similarity with sister species.

Typus. Czech Republic, forest near Sedlečko, Karlovy Vary region, fur of *Myodes glareolus*, 2019, *Š. Moulíková* (holotype PRM 954727, culture ex-type CCF 6387 = CGS12-4, mating-type gene idiomorph MAT1-2-1).

Vegetative mycelium consists of hyaline, smooth-walled, septate hyphae; spiral hyphae not observed. *Conidiophores* simple, conidiogenous hyphae unbranched or laterally branched max. two times. *Microconidia* hyaline, smooth-walled, non-septate, cylindrical to clavate, 3.5–17.5 (5.8 ± 2.4) × 1.5–2.5 (2 ± 0.2) µm. *Macroconidia* hyaline, smooth-walled, septate with two to four cells, cylindrical, 8.5–22 (14.5 ± 3.5) × 2–3.5 (2.4 ± 0.3) µm. *Ascomata* and *pseudoascomata* not observed.

Culture characteristics (after 14 d) — Colonies on MEA at 25 °C 25–26 mm diam, floccose, submerged margins, white to yellowish white (2A2), reverse yellowish white (4A2) with brownish orange centre (5C5). Colonies on SDA at 25 °C 28–30 mm diam, centre velvety to granular, surrounded by fine cottony mycelium with irregular margins, white to yellowish white (1A2), reverse yellowish white (4A2) with reddish yellow centre (4A6). Colonies on OA at 25 °C approximately 25 mm diam, centre granular, surrounded by cottony filamentous mycelium, white to yellowish white (2A2), with amber yellow (4B6) exudate in the centre, reverse yellowish white (4A2) with brownish orange centre (6C4). Colonies on PDA at 25 °C 21–24 mm diam, centre granular, surrounded by cottony mycelium, irregular margins, white to yellowish white (2A2), reverse greyish yellow (4B4) with light brown centre (5D5). No growth on MEA at 30 °C.

Ecology — The species was isolated from soil in a bat hibernaculum (Lorch et al. 2013) in the USA and rodents in the Czech Republic. Concerning the environmental samples, it was found only in one soil sample from a forest habitat in British Columbia (Canada) (Sukdeo et al. 2018) and in two soil samples from tundra in Colorado (USA) (Porazinska et al. 2018, Farrer et al. 2019).

Additional isolate examined. USA, Massachusetts, soil from bat hibernaculum, 2008/2009, *J.M. Lorch* (CCF 6281 = 07MA15).

Notes — *Arthroderma simile* is phylogenetically related to *A. insingulare* and *A. rodenticum*. For distinguishing characters see description of *A. rodenticum*.

Arthroderma psychrophilum Moulikova, Hubka, J.M. Lorch, Kubátová & Cmokova, *sp. nov.* — MycoBank MB 845986; Fig. 8

Etymology. Greek, *psy - chro´- phil - um*, referring to *psychros* (cold) and *philos* (loving), cold-loving (psychrophilic) growth.

Typus. USA, Wisconsin, Grant County, wing skin of hibernating *Myotis lucifugus*, 2013, *J.P. White* & *J.M. Lorch* (holotype PRM 955279, culture ex-type CCF 5960 = NWHC 44738-022_I3 (44738-22-I1-SD)).

Vegetative mycelium consists of hyaline, smooth-walled, septate hyphae; spiral hyphae not observed. *Conidiophores* simple, conidiogenous hyphae unbranched or laterally branched max. two times. *Microconidia* hyaline, non-septate, sessile on the conidiogenous hyphae, often on the lateral protrusions of the hyphae, solitary, obovate to pyriform, smooth-walled, a part of conidia becoming verrucose at maturity, 4–7 (5.4 ± 0.7) × 3–4.5 (3.8 ± 0.5) µm. *Macroconidia* absent. *Ascomata*, *pseudoascomata* and *peridial hyphae* not observed.

Culture characteristics (after 14 d) — Colonies on MEA at 15 °C 13–29 mm diam, cottony to floccose (submerged in strain CCF 6136), margins filamentous to submerged, white, yellowish white (3A2) to light orange (5A5) with white to yellow (3A6) margins, reverse light orange (5A5) to dull yellow (3B3) with greyish yellow (4B4) to yellow (3A6) margins. Colonies on SDA at 15 °C 12–30 mm diam, cottony to floccose (velvety in strain CCF 6136), margins filamentous, yellowish white (3A2), pale yellow (2A3) to yellowish orange (4A7) with white margins, reverse greyish yellow (4B4), reddish yellow (4A6) to deep orange (5A8) with light yellow (4A4) to yellow (3A6) marginal parts. Colonies on OA at 15 °C 9–34 mm diam, cottony to floccose (submerged in strain CCF 6136), margins filamentous, pale yellow (2A3) to deep orange (5A8) in the centre, marginal parts white to yellow (3A6), reverse greyish yellow (4B4, 4B6) to dark orange (5B8). Colonies on PDA at 15 °C 12–28 mm

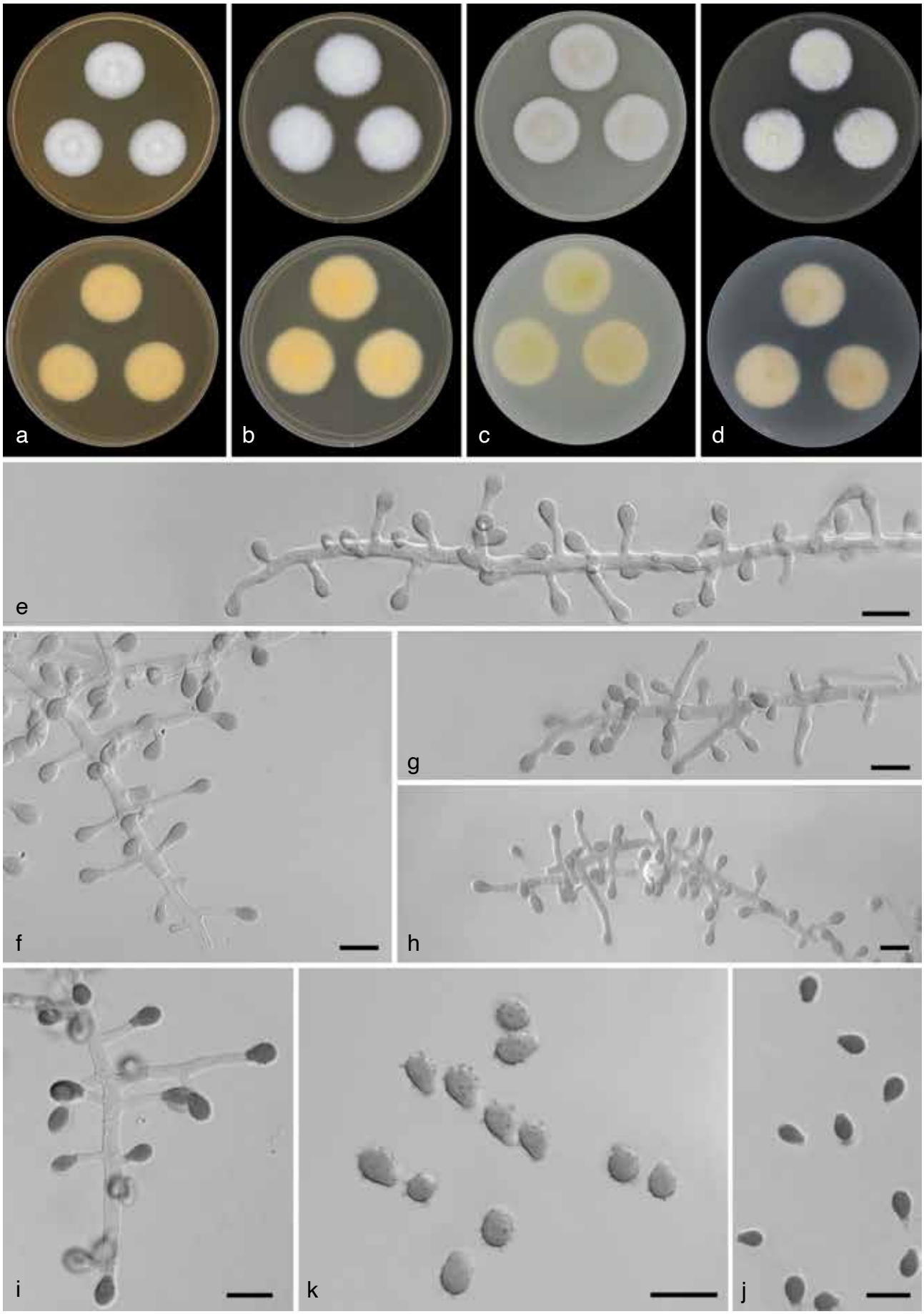

Fig. 8 *Arthroderma psychrophilum* sp. nov. a–b. Colonies after 2 wk at 25 °C on malt extract agar (a), Sabouraud's dextrose agar (b), oatmeal agar (c), potato dextrose agar (d); e–i. conidiophores; k. mature, verrucose, obovate to pyriform microconidia; j. smooth-walled, obovate to pyriform microconidia. — Scale bars: 10 µm.

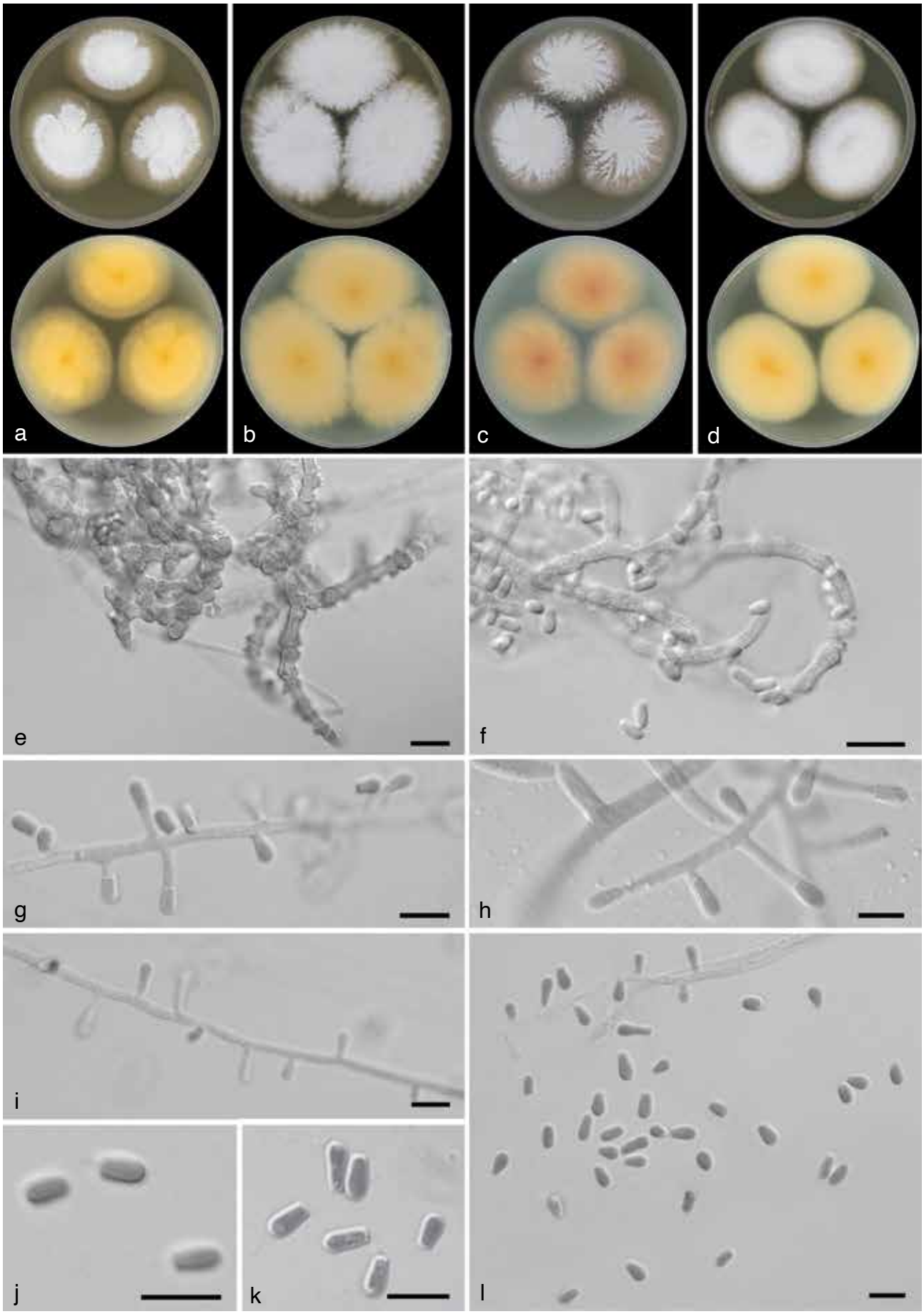

Fig. 9 *Arthroderma zoogenum* sp. nov. a–b. Colonies after 2 wk at 25 °C on malt extract agar (a), Sabouraud's dextrose agar (b), oatmeal agar (c), potato dextrose agar (d); e–f. hyaline, hooked peridial hyphae occurring on pseudoascomata, with dumbbell-shaped, gently echinulate peridial cells; g–i. sparsely branched conidiophores; j–l. smooth-walled, cylindrical to clavate microconidia. — Scale bars: 10 µm.

diam, cottony to floccose (velvety in strain CCF 6136), margins filamentous, light yellow (2A5), pale yellow (2A3) to yellowish orange (4A7) in the centre, marginal parts white, reverse pastel yellow (3A4), yellow (3A6, 3A7), greyish yellow (4B4) to deep orange (5A8). The colony diameters of the isolate CCF 6136 were approximately half in comparison with other examined strains. The isolates lost their ability to grow at 25 °C after reinoculation.

Ecology — *Arthroderma psychrophilum* is associated with small, free-living mammals (bats, rodents) in the Czech Republic and the USA. The GlobalFungi Database did not contain any sequences that could be assigned to this species.

Additional isolates examined. Czech Republic, farm in Hartoušov, near Cheb, fur of *Mus musculus*, 2019, *Š. Moulíková* (CCF 6422); ibid. (CCF 6424); farm in Loužek, near Cheb, fur of *Mus musculus*, 2019, *Š. Moulíková* (CCF 6423); Bohemian Karst, air in an underground tunnel of Velká Amerika quarry (tunnel is populated by abundant bat colony), 2014, *A. Kubátová* (CCF 5856 = CCF 6136).

Notes — *Arthroderma psychrophilum* is phylogenetically related to *A. oceanitis* and *A. silverae.* In contrast to *A. psychrophilum*, *A. oceanitis* is capable of growing at 25 °C and has larger conidia (7–17 × 4–10 µm), which are coarsely verrucose to asperulate (Crous et al. 2013). *Arthroderma silverae* is a homothallic species that is also capable of growing at 25 °C (Currah et al. 1996).

Arthroderma zoogenum Moulikova, Hubka, J.M. Lorch, Ovchinnikov & Cmokova, *sp. nov.* — MycoBank MB 845987; Fig. 9

Etymology. Latin, *zoogenum*, referring to the isolation of species from various animals.

Typus. Czech Republic, forest near Sedlečko, Karlovy Vary region, fur of *Myodes glareolus*, 2019, *Š. Moulíková* (holotype PRM 955282, culture ex-type CCF 6382 = CGS2-5, mating-type gene idiomorph MAT1-1-1).

Vegetative mycelium consists of hyaline, smooth-walled, septate hyphae; spiral hyphae not observed on vegetative mycelium, only rarely in association with peridial hyphae. *Conidiophores* simple, conidiogenous hyphae unbranched or laterally branched max. two times. *Microconidia* hyaline, smooth-walled, non-septate, clavate, 3–6 (4.1 ± 0.6) × 1.5–2.5 (2 ± 0.2) µm. *Macroconidia* not observed. *Pseudoascomata* consisting of clusters of conidiophores and peridial hyphae. *Peridial hyphae* hyaline, hooked; *peridial cells* dumbbell-shaped, echinulate.

Culture characteristics (after 14 d) — Colonies on MEA at 25 °C 41–49 mm diam, floccose to granular, white to yellowish white (2A2 to 3A2), reverse yellowish white (4A2), reddish yellow (4A6) to light brown (5D6). Colonies on SDA at 25 °C 52–61 mm diam, floccose to granular, centrally raised, white to yellowish white (3A2), reverse light yellow (4A4) to reddish golden (6C7) or reddish yellow (4B7). Colonies on OA at 25 °C 43–48 mm diam, floccose to granular, white, pale yellow (3A3) to yellowish white (4A2), reverse pale yellow (4A3, 4A4) to reddish yellow (4A6) with brown centre (6D7). Colonies on PDA at 25 °C 44–51 mm diam, coarsely granular, centrally raised, white to pale white (3A3), reverse yellowish white (3A2) to reddish yellow (4A6). Colonies on MEA at 30 °C 35–38 mm diam, floccose, centrally raised, margins submerged, white to pale yellow, reverse pale yellow (4A3) with apricot yellow centre (5B6). No growth on MEA at 37 °C.

Ecology — Aside from the studied material, the strains IFM 41172 (Finland, from *Meles meles*, 1990, isol. R. Aho) and VMZ Sob1.1-19 (Russia, Siberia Region, skin lesions in wild *Martes zibellina*, 2019, isol. R.S. Ovchinnikov, MAT1-1-1) belong to this species phylogenetically. The species was isolated from various animals (badger, sable, timber rattlesnake, bank vole) in geographically distant places in the world (USA, Czech Republic, Finland, and Siberia). Concerning the metabarcoding data, *A. zoogenum* was found in two soil samples collected in forest habitat in Switzerland (Merges et al. 2018).

Additional isolates examined. Finland, *Meles meles* (badger), 1990, *R. Aho* (IFM 41172). – Russia, Siberia Region, skin lesions in wild *Martes zibellina* (sable), 2019, *R.S. Ovchinnikov* (VMZ Sob1.1-19), MAT1-1-1. – USA, Massachusetts, skin of *Crotalus horridus* (timber rattlesnake), 2013, *J. Condon* & *J.M. Lorch* (CCF 5959 = NWHC 44736-13-C4-I1), MAT1-2-1.

Notes — This species is phylogenetically related to *A. cuniculi*, *A. tuberculatum*, and *A. phaseoliforme*. In comparison with *A. cuniculi* and *A. phaseoliforme*, *A. zoogenum* does not produce macroconidia. Compared to *A. phaseoliforme* and *A. tuberculatum*, *A. zoogenum* produces smooth-walled, clavate microconidia, whereas microconidia of *A. phaseoliforme* are reniform and *A. tuberculatum* produces significantly larger, ovoid and echinulate microconidia: 5.5–21.5 (10.8 ± 2.9) × 4–12 (7.4 ± 1.6) µm. *Arthroderma zoogenum* grows slower on OA at 25 °C and faster on MEA at 30 °C in comparison with *A. cuniculi* (OA: 50–61 mm, MEA at 30 °C: 20–30 mm), while faster on PDA at 25 °C and slower on MEA at 30 °C in comparison with *A. tuberculatum* (PDA: 40–41 mm, MEA at 30 °C: 40–42 mm). By contrast, *A. phaseoliforme* grows the fastest on all cultivation media (MEA: 63–66 mm, SDA: 68 mm, OA: 60–61 mm, PDA: 60–62 mm, MEA at 30 °C: 51–52 mm).

DISCUSSION

In this study, we focused on screening wild rodents for the presence of dermatophytes. A wide variety of dermatophytes, including geophilic *Arthroderma* and *Nannizzia* and zoophilic *Trichophyton* and *Microsporum* species, have been previously reported from rodents (Mantovani et al. 1982, Gallo et al. 2005, Papini et al. 2008). However, the taxonomy of dermatophytes has been revised numerous times and it is often problematic to reassign accurate species identifications to historical samples. Among our strains isolated from small wild rodents, we did not detect zoophilic *Trichophyton* and *Microsporum* species. Similarly, we did not isolate geophilic dermatophytes outside the genus *Arthroderma.*

Phylogenetic analyses revealed the presence of four previously described and four new species of *Arthroderma* among our 29 isolates recovered from wild rodents. Of the previously described species, three – *A. quadrifidum* (often referred to in the historical literature as *T. terrestre*) (Alteras 1966, Smith et al. 1969, Knudtson & Robertstad 1970, Houin et al. 1972, Hubálek et al. 1979, Mantovani et al. 1982, Gallo et al. 2005, Papini et al. 2008), *A. curreyi* and *A. cuniculi* (Knudtson & Robertstad 1970, Hubálek et al. 1979, Chabasse et al. 1987) – had been previously reported from various rodent species in Europe and North America, whereas we report *A. crocatum* from rodents for the first time.

Based upon our proposal of new species, species diversity within the genus *Arthroderma* increased from 27 (Hainsworth et al. 2021) to 31 recognised species (an increase of 13 %). The diversity we detected was unexpectedly high given that we sampled a single type of substrate (rodent fur) in a limited geographic area (Czech Republic) using a culture-based approach, and it is highly probable that we did not fully characterise the diversity of *Arthroderma* species from our study population (Fig. 2). When comparing rodent species, bank voles hosted the highest species diversity of *Arthroderma* in comparison with both house mice and yellow-necked mice (even those inhabiting the same locality as the voles). The differences observed in *Arthroderma* species diversity can probably be explained by different ecological niches of these rodents. House mice live predominantly in association with human settlements (often in or

around buildings), yellow-necked mice occupy the undergrowth of forests and gardens, and bank voles occur in wild habitats and spend a considerable amount of time underground (in direct contact with soil).

Soil environments are relatively stable with respect to temperature fluctuations and surface changes, and soil is thought to be the primary habitat in which sexual recombination of dermatophytes takes place (Gräser et al. 2006). However, the role of different soil types, presence of a keratin source, and role of animals in the life cycle of dermatophytes warrants further investigation. To explore biogeography and ecological significance of the soil environment for *Arthroderma*, we searched published datasets originating from both the culture-based (NCBI GenBank database) and molecular-based (GlobalFungi) studies. Based on phylogenetic trees (generated from ITS1 or ITS2 sequence data), most of the phylotypes contain the reference sequences of already known species, had relatively low intraspecific genetic variability (≥ 98.8 %) and corresponded to a single species. On the other hand, other phylotypes, such as *A. quadrifidum*, *A. insingulare*, and *A. crocatum*, can be considered as phylogenetic lineages of uncertain taxonomic level (i.e., potentially consisting of several cryptic species) due to high genetic variability within the taxa. Based on the metabarcoding data, we observed that some *Arthroderma* lineages/species were frequently detected in soil samples (Fig. 3, red and orange taxa) and thus soil may serve as an important reservoir for these taxa. Other taxa were poorly represented in datasets from soil studies (Fig. 3, black taxa), which may indicate that these species utilise other substrates as reservoirs. The GlobalFungi Database contained data primarily generated from molecular analyses of soil, root, shoot, and dead wood samples (Fig. 4b). Substrates relevant for *Arthroderma* spp., such as keratin rich soils (Dawson 1963, Weitzman & Summerbell 1995), bird nests (Otcenášek et al. 1967, Hubálek 1970), animal faeces (Kuehn 1960, Currah et al. 1996), or caves (Kajihiro 1965, Evolceanu & Alteraş 1967, Zeller 1970, Lorch et al. 2013, 2015) were not well-represented in the GlobalFungi Database. Overall, the majority of *Arthroderma* diversity originated from strains/sequences associated with animal substrates, while the number of phylotypes identified from soil samples was low (Fig. 3). The relative rarity of *Arthroderma* in soil detected by molecular techniques is consistent with the infrequency in which some species of *Arthroderma* are cultivated from soil samples (Chabasse 1988, Nováková et al. 2012) and the finding that some species appear to be weak competitors in soil lacking keratin (Pugh 1964).

We noted that detections of some species of *Arthroderma* were geographically restricted. For example, *A. rodenticum* was absent in datasets from Western and Northern Europe (Scandinavian Peninsula), even though these regions are very well represented in the GlobalFungi Database (Fig. 4a, grey dots). Such a distribution pattern is unexpected for ubiquitous soil fungi but may be more consistent with fungi closely tied to particular animals. However, the geographical distribution of the bank vole does not mirror the detection pattern of *A. rodenticum* as this rodent is also distributed across Scandinavia (Cook et al. 2004). Therefore, other factors, such as environmental conditions, may play a role in the distribution of *Arthroderma* species.

In contrast to low abundance of *Arthroderma* in soil samples, prevalence of *Arthroderma* in the rodents sampled for this study was high (15–71 %). Prevalence of the most common species, *A. rodenticum*, was around 57 % at the study site. The prevalence of *A. rodenticum* was comparable to or even higher than those reported for zoophilic dermatophytes such as *T. erinacei*, which has a prevalence 20–45 % in free living hedgehog populations (Smith & Marples 1964, Morris & English 1969, Gregory & English 1975, Gregory et al. 1978, Gnat et al. 2022, Le Barzic et al. 2021) and *A. quadrifidum* (*T. terrestre*), which has a prevalence of 6–42 % in rodents (Houin et al. 1972, Hubálek et al. 1979, Chabasse et al. 1987, Gallo et al. 2005). Such a high prevalence may indicate very close association with animal hosts and suggest that *A. rodenticum* is either a commensal or pathogen. However, pathogenic potential of *Arthroderma* species in wild mammals has never been rigorously investigated. The one exception is *A. redellii*, which causes dermatophytosis in hibernating bats (Lorch et al. 2015).

Many *Arthroderma* species are thought to be non-pathogenic to mammals because they are incapable of growth at 37 °C (Robert & Casadevall 2009). Indeed, it is plausible that many *Arthroderma* species closely associated with animals are non-pathogenic commensals that derive energy from dead skin cells, shed hair, and other keratinaceous material without actively infecting the host. However, the potential for *Arthroderma* species to act as pathogens warrants further investigation. Fungi with optimal temperature below 37 °C may still be able to infect superficial tissues and distal body parts that have a significantly lower temperature, or infect animals during hibernation. This is true for the non-dermatophyte species *Malbranchea ostraviensis* (syn. *Auxarthron ostraviense*), which is a well-documented cause of human infections but is unable to grow above 35 °C (Hubka et al. 2013). Moreover, pathogenic dermatophytes that have coevolved with their hosts are usually asymptomatic and do not cause clinical disease in healthy individuals (Drouot et al. 2009, Kupsch et al. 2017, Le Barzic et al. 2021). In addition, *A. crocatum* and *A. quadrifidum* (frequently misidentified as *T. terrestre*) that were isolated in this study from wild rodents have repeatedly been reported from human clinical material (L'Ollivier et al. 2013, Nenoff et al. 2013, Hubka et al. 2014b, Hainsworth et al. 2020, Brasch et al. 2021). Among the newly described species, *A. rodenticum*, reported as *Arthroderma* sp. bM 128 by De Respinis et al. (2013), was found on unspecified clinical material. Other *Arthroderma* species such as *A. eboreum* (syn. *A. olidum*), *A. thuringiense*, and *A. chiloniense* have also been occasionally reported from both substrates associated with animals (rodents and badger burrows), as well as clinical material (Brasch & Gräser 2005, Nenoff et al. 2014, Brasch et al. 2019). The importance of *Arthroderma* species as pathogens may be currently underestimated due to difficulties in isolating and identifying these organisms and *a priori* assumptions by many clinicians that they are non-pathogenic or secondary pathogens. Awareness of these species in the clinical setting is growing with the increasing use of molecular methods for species identification (Hubka et al. 2014a, Brasch et al. 2021). However, histopathologic verification of human infections is rarely performed to confirm pathogenicity.

Investigation of the pathogenic potential for *Arthroderma* species that exhibit optimal growth at lower temperatures (20–25 °C, e.g., newly described species *A. psychrophilum*) would be beneficial. Although the ecology of *A. psychrophilum* is poorly known, its isolation from environments occupied by hibernating bats could suggest it is capable of infecting torpid mammals, similar to the psychrophilic fungi *A. redellii* (Lorch et al. 2015) and *Pseudogymnoascus destructans* (Lorch et al. 2011).

In this study, we documented a high diversity of *Arthroderma* on wild rodents. For the first time, we also demonstrated the application of the GlobalFungi Database in studying habitat preferences and distributions of dermatophytic fungi. To fully understand the ecology and phylogeography of the genus *Arthroderma*, material from certain keratin-rich (animal-associated) sources would need to be screened and soil environmental conditions (e.g., pH, composition, moisture, temperature, keratin abundance) would need to be better documented.

Acknowledgements The project was supported by the Czech Ministry of Health (grant NU21-05-00681), the Charles University Research Centre program no. 204069, and Czech Academy of Sciences Long-term Research Development Project RVO: 61388971. We thank Alena Kubátová for providing photos from scanning electron microscopy (SEM) and Jana Nebesářová for technical assistance with SEM. We thank Milada Chudíčková and Soňa Kajzrová for their invaluable assistance in the laboratory and Karel Švec for help with figure design. We also thank Lucie Nováková, Tereza Matějková, Pavel Stopka, Miloš Macholán, and Zuzana Hiadlovská for their help with capturing rodents. The research reported in this publication was part of the long-term goals of the ISHAM Onygenales working group. We thank Takashi Yaguchi and Sayaka Ban from Medical Mycology Research Center (Chiba University, Japan) for supplying data related to isolate IFM 41172. Any use of trade, firm, or product names is for descriptive purposes only and does not imply endorsement by the U.S. Government.

Declaration on conflict of interest The authors declare that there is no conflict of interest.

REFERENCES

Alteras I. 1966. Human dermatophyte infections from laboratory animals. Sabouraudia: Journal of Medical and Veterinary Mycology 4: 143–145.

Anthony M, Frey S, Stinson K. 2017. Fungal community homogenization, shift in dominant trophic guild, and appearance of novel taxa with biotic invasion. Ecosphere 8: e01951.

Bahram M, Netherway T, Hildebrand F, et al. 2020. Plant nutrient-acquisition strategies drive topsoil microbiome structure and function. New Phytologist 227: 1189–1199.

Baldrian P, Zrůstová P, Tláskal V, et al. 2016. Fungi associated with decomposing deadwood in a natural beech-dominated forest. Fungal Ecology 23: 109–122.

Brasch J, Beck-Jendroschek V, Voss K, et al. 2019. Arthroderma chiloniense sp. nov. isolated from human stratum corneum: description of a new Arthroderma species. Mycoses 62: 73–80.

Brasch J, Beck-Jendroschek V, Voss K, et al. 2021. Arthroderma crocatum auf menschlicher Haut. Der Hautarzt 72: 267–270.

Brasch J, Gräser Y. 2005. Trichophyton eboreum sp. nov. isolated from human skin. Journal of Clinical Microbiology 43: 5230–5237.

Chabasse D. 1988. Taxonomic study of keratinophilic fungi isolated from soil and some mammals in France. Mycopathologia 101: 133–140.

Chabasse D, Guiguen C, Couatarmanac'h A, et al. 1987. Contribution à la connaissance de la flore fongique kératinophile isolée des petits mammifères sauvages et du lapin de garenne en France-Discussion sur les espèces fongiques rencontrées. Annales de Parasitologie Humaine et Comparée 62: 357–368.

Chmel L, Buchvald J, Kleibl K. 1967. Die Rolle der Naturfaktoren bei Entstehung der Naturherde der Dermatomykosen. Mycoses 10: 263–270.

Chmel L, Buchvald J, Valentova M. 1975. Spread of Trichophyton mentagrophytes var. gran. infection to man. International Journal of Dermatology 14: 269–272.

Chollet A, Cattin V, Fratti M, et al. 2015. Which fungus originally was Trichophyton mentagrophytes? Historical review and illustration by a clinical case. Mycopathologia 180: 1–5.

Čmoková A, Kolařík M, Dobiáš R, et al. 2020. Resolving the taxonomy of emerging zoonotic pathogens in the Trichophyton benhamiae complex. Fungal Diversity 104: 333–387.

Čmoková A, Rezaei-Matehkolaei A, Kuklová I, et al. 2021. Discovery of new Trichophyton members, T. persicum and T. spiraliforme spp. nov., as a cause of highly inflammatory tinea cases in Iran and Czechia. Microbiology Spectrum 9: e00284–00221.

Cook JA, Runck AM, Conroy CJ. 2004. Historical biogeography at the crossroads of the northern continents: molecular phylogenetics of red-backed voles (Rodentia: Arvicolinae). Molecular Phylogenetics and Evolution 30: 767–777.

Crous PW, Wingfield MJ, Guarro J, et al. 2013. Fungal Planet description sheets: 154–213. Persoonia 31: 188–296.

Currah R, Abbott SP, Sigler L. 1996. Arthroderma silverae sp. nov. and Chrysosporium vallenarense, keratinophilic fungi from arctic and montane habitats. Mycological Research 100: 195–198.

Dawson CO. 1963. Two new species of Arthroderma isolated from soil from rabbit burrows. Sabouraudia: Journal of Medical and Veterinary Mycology 2: 185–191.

De Hoog GS, Dukik K, Monod M, et al. 2017. Toward a novel multilocus phylogenetic taxonomy for the dermatophytes. Mycopathologia 182: 5–31.

De Respinis S, Tonolla M, Pranghofer S, et al. 2013. Identification of dermatophytes by matrix-assisted laser desorption/ionization time-of-flight mass spectrometry. Sabouraudia: Journal of Medical and Veterinary Mycology 51: 514–521.

De Vroey C. 1964. Formes sexuées des dermatophytes. Production de cleistothèces de Microsporum gypseum (Bodin) Guiart et Grigorakis sur divers milieux stériles. Annales de la Société Belge de Médecine Tropicale 44: 831–840.

Drouot S, Mignon B, Fratti M, et al. 2009. Pets as the main source of two zoonotic species of the Trichophyton mentagrophytes complex in Switzerland, Arthroderma vanbreuseghemii and Arthroderma benhamiae. Veterinary Dermatology 20: 13–18.

Evolceanu R, Alteraş I. 1967. Eine keratinophile Chrysosporium-Art mit ausgesprochen dermatophytischen, immunbiologischen Eigenschaften aus Guano von einer Grotte in Rumänien (unvollkommenes Stadium von Arthroderma multifidum-Dawson 1963?) (Erste Mitteilung). Mycoses 10: 489–492.

Farrer EC, Porazinska DL, Spasojevic MJ, et al. 2019. Soil microbial networks shift across a high-elevation successional gradient. Frontiers in Microbiology 10: 2887.

Flowerdew JR, Shore RF, Poulton SM, et al. 2004. Live trapping to monitor small mammals in Britain. Mammal Review 34: 31–50.

Frøslev TG, Kjøller R, Bruun HH, et al. 2019. Man against machine: Do fungal fruitbodies and eDNA give similar biodiversity assessments across broad environmental gradients? Biological Conservation 233: 201–212.

Gallo MG, Lanfranchi P, Poglayen G, et al. 2005. Seasonal 4-year investigation into the role of the alpine marmot (Marmota marmota) as a carrier of zoophilic dermatophytes. Medical Mycology 43: 373–379.

Gams W. 2007. Biodiversity of soil-inhabiting fungi. Biodiversity and Conservation 16: 69–72.

Gardes M, Bruns TD. 1993. ITS primers with enhanced specificity for basidiomycetes-application to the identification of mycorrhizae and rusts. Molecular Ecology 2: 113–118.

Geml J. 2019. Soil fungal communities reflect aspect-driven environmental structuring and vegetation types in a Pannonian forest landscape. Fungal Ecology 39: 63–79.

Glass NL, Donaldson GC. 1995. Development of primer sets designed for use with the PCR to amplify conserved genes from filamentous ascomycetes. Applied and Environmental Microbiology 61: 1323–1330.

Gnat S, Łagowski D, Dyląg M, et al. 2022. European hedgehogs (Erinaceus europaeus L.) as a reservoir of dermatophytes in Poland. Microbial Ecology 84: 363–375.

Gräser Y, De Hoog S, Summerbell R. 2006. Dermatophytes: recognizing species of clonal fungi. Medical Mycology 44: 199–209.

Gregory M, English MP. 1975. Arthroderma benhamiae infection in the central African hedgehog, Erinaceus albiventris, and a report of a human case. Mycopathologia 55: 143–147.

Gregory M, Stockdale PM, English MP. 1978. Ringworm of the African hedgehog (Erinaceus albiventris) in the Ivory Coast due to Arthroderma benhamiae. Mycopathologia 66: 125–126.

Grin E, Ožegović L. 1963. Influence of the soil on certain dermatophytes and their evolutional trend. Mycopathologia et Mycologia Applicata 21: 23–28.

Guindon S, Delsuc F, Dufayard J-F, et al. 2009. Estimating maximum likelihood phylogenies with PhyML. Methods in Molecular Biology 537: 113–137.

Hainsworth S, Hubka V, Lawrie AC, et al. 2020. Predominance of Trichophyton interdigitale revealed in podiatric nail dust collections in Eastern Australia. Mycopathologia 185: 175–185.

Hainsworth S, Kučerová I, Sharma R, et al. 2021. Three-gene phylogeny of the genus Arthroderma: basis for future taxonomic studies. Medical Mycology 59: 355–365.

Hall T. 1999. BioEdit: a user-friendly biological sequence alignment editor and analysis program for Windows 95/98/NT. Nucleic Acids Symposium Series 41: 95–98.

Hamm PS, Mueller RC, Kuske CR, et al. 2020. Keratinophilic fungi: Specialized fungal communities in a desert ecosystem identified using cultured-based and Illumina sequencing approaches. Microbiological Research 239: 126530.

Hammer Ø, Harper DA, Ryan PD. 2001. PAST: Paleontological statistics software package for education and data analysis. Palaeontologia Electronica 4: 9.

Houin R, Rouget-Campana Y, Le Fichoux Y, et al. 1972. Isolement de Trichophyton mentagrophytes (Robin) Blanchard 1896, Nannizia persicolor Stockdale 1967 et Trichophyton terrestre Durie et Frey 1957, du pelage de Rongeurs-Essai d'interprétation écologique. Annales de Parasitologie Humaine et Comparée 47: 421–429.

Hubálek Z. 1970. Trichophyton georgiae Varsavsky et Ajello, from birds in Czechoslovakia and Yugoslavia. Sabouraudia: Journal of Medical and Veterinary Mycology 8: 1–3.

Hubálek Z. 2000. Keratinophilic fungi associated with free-living mammals and birds. In: Kushawaha RKS, Guarro J (eds), Biology of dermatophytes and other keratinophilic fungi: 86–92. Revista Iberoamericana de Micología, Bilbao, Spain.

Hubálek Z, Rosický B, Otčenášek M. 1979. Fungi on the hair of small wild mammals in Czechoslovakia and Yugoslavia. Česká Mykologie 33: 81–93.

Hubka V, Dobiasova S, Lyskova P, et al. 2013. Auxarthron ostraviense sp. nov., and A. umbrinum associated with non-dermatophytic onychomycosis. Medical Mycology 51: 614–624.

Hubka V, Mallátová N, Hamal P, et al. 2014a. Molekulární epidemiologie dermatofytóz v České republice: výsledky dvouleté studie. Česko-Slovenská Dermatologie 89: 167–174.

Hubka V, Nissen CV, Jensen RH, et al. 2015. Discovery of a sexual stage in Trichophyton onychocola, a presumed geophilic dermatophyte isolated from toenails of patients with a history of T. rubrum onychomycosis. Medical Mycology 53: 798–809.

Hubka V, Peano A, Čmoková A, et al. 2018. Common and emerging dermatophytoses in animals: well-known and new threats. In: Seyedmousavi S, De Hoog GS, Guillot J, et al. (eds), Emerging and epizootic fungal infections in animals. Springer, Switzerland: 31–79.

Hubka V, Větrovský T, Dobiášová S, et al. 2014b. Molekulární epidemiologie dermatofytóz v České republice – výsledky dvouleté studie. Česko-Slovenská Dermatologie 89: 167–174.

Ibbotson R, Pugh G. 1975. Use of the fluorescent antibody technique for the evaluation of Arthroderma uncinatum in soil. Mycopathologia 56: 119–123.

Kajihiro ES. 1965. Occurrence of dermatophytes in fresh bat guano. Applied Microbiology 13: 720–724.

Katoh K, Rozewicki J, Yamada KD. 2019. MAFFT online service: multiple sequence alignment, interactive sequence choice and visualization. Briefings in Bioinformatics 20: 1160–1166.

Knudtson WU, Robertstad GW. 1970. The isolation of keratinophilic fungi from soil and wild animals in South Dakota. Mycopathologia et Mycologia Applicata 40: 309–323.

Kornerup A, Wanscher J. 1978. Methuen handbook of colour. 3rd edn, Eyre Methuen. United Kingdom.

Krebs CJ. 1989. Ecological methodology. Harper & Row, New York, NY, USA.

Kuehn HH. 1960. Observations on Gymnoascaceae. VIII. A new species of Arthroderma. Mycopathologia et Mycologia Applicata 13: 189–197.

Kupsch C, Berlin M, Gräser Y. 2017. Dermophytes and guinea pigs: An underestimated danger? Der Hautarzt 68: 827–830.

L'Ollivier C, Cassagne C, Normand A-C, et al. 2013. A MALDI-TOF MS procedure for clinical dermatophyte species identification in the routine laboratory. Medical Mycology 51: 713–720.

Lanfear R, Frandsen PB, Wright AM, et al. 2017. PartitionFinder 2: new methods for selecting partitioned models of evolution for molecular and morphological phylogenetic analyses. Molecular Biology and Evolution 34: 772–773.

Le Barzic C, Čmoková A, Denaes C, et al. 2021. Detection and control of dermatophytosis in wild European hedgehogs (Erinaceus europaeus) admitted to a French wildlife rehabilitation centre. Journal of Fungi 7: 74.

Lorch JM, Lindner DL, Gargas A, et al. 2013. A culture-based survey of fungi in soil from bat hibernacula in the eastern United States and its implications for detection of Geomyces destructans, the causal agent of bat white-nose syndrome. Mycologia 105: 237–252.

Lorch JM, Meteyer CU, Behr MJ, et al. 2011. Experimental infection of bats with Geomyces destructans causes white-nose syndrome. Nature 480: 376–378.

Lorch JM, Minnis AM, Meteyer CU, et al. 2015. The fungus Trichophyton redellii sp. nov. causes skin infections that resemble white-nose syndrome of hibernating bats. Journal of Wildlife Diseases 51: 36–47.

Lysková P, Dobiáš R, Čmoková A, et al. 2021. An outbreak of Trichophyton quinckeanum zoonotic infections in the Czech Republic transmitted from cats and dogs. Journal of Fungi 7: 684.

Mantovani A. 1978. The role of animals in the epidemiology of the mycoses. Mycopathologia 65: 61–66.

Mantovani A, Morganti L, Battelli G, et al. 1982. The role of wild animals in the ecology of dermatophytes and related fungi. Folia Parasitologica 29: 279–284.

Mašínová T, Bahnmann BD, Větrovský T, et al. 2017. Drivers of yeast community composition in the litter and soil of a temperate forest. FEMS Microbiology Ecology 93: fiw223.

Matějková T, Hájková P, Stopková R, et al. 2020. Oral and vaginal microbiota in selected field mice of the genus Apodemus: a wild population study. Scientific Reports 10: 1–11.

McKeever S, Menges R, Kaplan W, et al. 1958. Ringworm fungi of feral rodents in southwestern Georgia. American Journal of Veterinary Research 19: 969–972.

Menges RW, Love GJ, Smith WW, et al. 1957. Ringworm in wild animals in southwestern Georgia. American Journal of Veterinary Research 18: 672–677.

Merges D, Bálint M, Schmitt I, et al. 2018. Spatial patterns of pathogenic and mutualistic fungi across the elevational range of a host plant. Journal of Ecology 106: 1545–1557.

Mirhendi H, Makimura K, De Hoog GS, et al. 2015. Translation elongation factor 1-α gene as a potential taxonomic and identification marker in dermatophytes. Medical Mycology 53: 215–224.

Moretti A, Agnetti F, Mancianti F, et al. 2013. Dermatophytosis in animals: epidemiological, clinical and zoonotic aspects. Giornale Italiano di Dermatologia e Venereologia 148: 563–572.

Morris P, English MP. 1969. Trichophyton mentagrophytes var. erinacei in British hedgehogs. Sabouraudia: Journal of Medical and Veterinary Mycology 7: 122–128.

Moudra A, Niederlova V, Novotny J, et al. 2021. Phenotypic and clonal stability of antigen-inexperienced memory-like T cells across the genetic background, hygienic status, and aging. The Journal of Immunology 206: 2109–2121.

Needle DB, Gibson R, Hollingshead NA, et al. 2019. Atypical dermatophytosis in 12 North American porcupines (Erethizon dorsatum) from the northeastern United States 2010–2017. Pathogens 8: 171.

Nenoff P, Erhard M, Simon JC, et al. 2013. MALDI-TOF mass spectrometry-a rapid method for the identification of dermatophyte species. Medical Mycology 51: 17–24.

Nenoff P, Winter I, Krueger C, et al. 2014. Trichophyton thuringiense H.A. Koch 1969. Ein seltener geophiler Dermatophyt, erstmals vom Menschen isoliert (Trichophyton thuringiense H.A. Koch 1969. A rare geophilic dermatophyte – now isolated for the first time from man). Hautarzt 65: 221–228.

Nguyen L-T, Schmidt HA, Von Haeseler A, et al. 2015. IQ-TREE: a fast and effective stochastic algorithm for estimating maximum-likelihood phylogenies. Molecular Biology and Evolution 32: 268–274.

Nilsson RH, Larsson K-H, Taylor AFS, et al. 2019. The UNITE database for molecular identification of fungi: handling dark taxa and parallel taxonomic classifications. Nucleic Acids Research 47: D259–D264.

Nováková A, Šimonovičová A, Kubátová A. 2012. List of cultivable microfungi recorded from soils, soil related substrates and underground environment of the Czech and Slovak Republics. Mycotaxon 119: 1–186.

O'Donnell K. 1993. Fusarium and its near relatives. In: Reynolds DR, Taylor JW (eds), The fungal holomorph: mitotic, meiotic and pleomorphic speciation in fungal systematics. CAB International, UK.

Oja J, Vahtra J, Bahram M, et al. 2017. Local-scale spatial structure and community composition of orchid mycorrhizal fungi in semi-natural grasslands. Mycorrhiza 27: 355–367.

Otčenášek M, Hudec K, Hubálek Z, et al. 1967. Keratinophilic fungi from the nests of birds in Czechoslovakia. Sabouraudia: Journal of Medical and Veterinary Mycology 5: 350–354.

Papini R, Nardoni S, Ricchi R, et al. 2008. Dermatophytes and other keratinophilic fungi from coypus (Myocastor coypus) and brown rats (Rattus norvegicus). European Journal of Wildlife Research 54: 455–459.

Porazinska DL, Farrer EC, Spasojevic MJ, et al. 2018. Plant diversity and density predict belowground diversity and function in an early successional alpine ecosystem. Ecology 99: 1942–1952.

Prada-Salcedo LD, Goldmann K, Heintz-Buschart A, et al. 2021. Fungal guilds and soil functionality respond to tree community traits rather than to tree diversity in European forests. Molecular Ecology 30: 572–591.

Pugh G. 1964. Dispersal of Arthroderma curreyi by birds, and its role in the soil. Sabouraudia: Journal of Medical and Veterinary Mycology 3: 275–278.

Purahong W, Wubet T, Lentendu G, et al. 2018. Determinants of deadwood-inhabiting fungal communities in temperate forests: molecular evidence from a large scale deadwood decomposition experiment. Frontiers in Microbiology 9: 2120.

Rambaut A. 2020. FigTree v. 1.4. 4. 2018. http://tree.bio.ed.ac.uk/software/figtree/ accessed February 2021.

Rambaut A, Drummond AJ, Xie D, et al. 2018. Posterior summarization in Bayesian phylogenetics using Tracer 1.7. Systematic Biology 67: 901–904.

R Core Team. 2020. R: A language and environment for statistical computing. (4.0.5). R Foundation for Statistical Computing, Vienna, Austria. http://www.R-project.org/ accessed January 2021.

Réblová M, Kolařík M, Nekvindová J, et al. 2021a. Phylogeny, global biogeography and pleomorphism of Zanclospora. Microorganisms 9: 706.

Réblová M, Kolařík M, Nekvindová J, et al. 2021b. Phylogenetic reassessment, taxonomy, and biogeography of Codinaea and similar fungi. Journal of Fungi 7: 1097.

Robert VA, Casadevall A. 2009. Vertebrate endothermy restricts most fungi as potential pathogens. The Journal of Infectious Diseases 200: 1623–1626.

Ronquist F, Teslenko M, Van Der Mark P, et al. 2012. MrBayes 3.2: efficient Bayesian phylogenetic inference and model choice across a large model space. Systematic Biology 61: 539–542.
Sayers EW, Cavanaugh M, Clark K, et al. 2019. GenBank. Nucleic Acids Research 47: D94–D99.
Sklenář F, Jurjević Ž, Houbraken J, et al. 2021. Re-examination of species limits in Aspergillus section Flavipedes using advanced species delimitation methods and description of four new species. Studies in Mycology 99: 100120.
Smith J, Marples MJ. 1964. Trichophyton mentagrophytes var. erinacei. Sabouraudia: Journal of Medical and Veterinary Mycology 3: 1–10.
Smith JM, Rush-Munro F, McCarthy M. 1969. Animals as a reservoir of human ringworm in New Zealand. Australasian Journal of Dermatology 10: 169–182.
Sukdeo N, Teen E, Rutherford PM, et al. 2018. Selecting fungal disturbance indicators to compare forest soil profile re-construction regimes. Ecological Indicators 84: 662–682.
Symoens F, Jousson O, Packeu A, et al. 2013. The dermatophyte species Arthroderma benhamiae: intraspecies variability and mating behaviour. Journal of Medical Microbiology 62: 377–385.
Uhrlaß S, Schroedl W, Mehlhorn C, et al. 2018. Molecular epidemiology of Trichophyton quinckeanum – a zoophilic dermatophyte on the rise. JDDG: Journal der Deutschen Dermatologischen Gesellschaft 16: 21–32.
Umnova I, Fomenko V. 1960. Trikhofitija poljovijkh miskei, vizvavshaja zarazenih ljudjeji (Trichophytosis in field mice causing infection in man). Vestnik Dermatologii i Venerologii 11: 36–38.
Větrovský T, Baldrian P, Morais D. 2018. SEED 2: a user-friendly platform for amplicon high-throughput sequencing data analyses. Bioinformatics 34: 2292–2294.
Větrovský T, Kohout P, Kopecký M, et al. 2019. A meta-analysis of global fungal distribution reveals climate-driven patterns. Nature Communications 10: 1–9.
Větrovský T, Morais D, Kohout P, et al. 2020. GlobalFungi, a global database of fungal occurrences from high-throughput-sequencing metabarcoding studies. Scientific Data 7: 1–14.
Villesen P. 2007. FaBox: an online toolbox for fasta sequences. Molecular Ecology Notes 7: 965–968.
Weitzman I, Summerbell RC. 1995. The dermatophytes. Clinical Microbiology Reviews 8: 240–259.
White TJ, Burns T, Lee S, et al. 1990. Amplification and direct sequencing of fungal ribosomal RNA genes for phylogenetics. In: Innis MA, Gelfand DH, Sninsky JJ, et al. (eds), PCR protocols: a guide to methods and applications: 282–287. Academic Press, USA.
Zeller L. 1970. Arthroderma species from the 'Baradla' cave in Aggtelek (Biospeologica Hungarica XXXI.). Annales of the University of Sciences Budapest, Section Biology 5: 273–280.

Supplementary material

Table S1 The biogeography, substrate, and habitat affinity of newly described *Arthroderma* species inferred from the GlobalFungi Database (ITS1 and ITS2 data). The same information, based on the ITS2 marker only, is provided for phylotypes identified in Fig. 3. The summary of geographical location, substrate, and habitat type is provided as a list of all studies in the database. Table is available via https://doi.org/10.5281/zenodo.7579684 or upon request.

Table S2 List of sequences used in the construction of the phylogenetic trees in Fig. 3, Appendix 2. Table is available via https://doi.org/10.5281/zenodo.7579684 or upon request.

Appendix 1 Primers combinations used in this study to amplify target DNA loci and determine mating-type gene idiomorphs.

Gene	Forward primer	Sequence (5'–3')	Reverse primer	Sequence (5'–3')	Reference
ITS rDNA	ITS1F	CTTGGTCATTTAGAGGAAGTA	ITS4	TCCTCCGCTTATTGATATGC	White et al. (1990), Gardes & Bruns (1993)
			NL4	GGTCCGTGTTTCAAGACGG	O'Donnell (1993)
tubb	Bt2a	GGTAACCAAATCGGTGCTGCTTTC	Bt2b	ACCCTCAGTGTAGTGACCCTTGGC	Glass & Donaldson (1995)
tef1-α	EF-DermF	CACATTAACTTGGTCGTTATCG	EF-DermR	CATCCTTGGAGATACCAGC	Mirhendi et al. (2015)
MAT1-1-1	ART-MAT1F1	TCAAGTCTGGACTGCTTCG	ART-MAT1R1	ACAATTCCAATGAADGGCMCA	This study
MAT1-2-1	ART-MAT2F1	TCCTTTGGCAGCATGCGATG	ART-MAT2R1	ACGCTATCCTCAAACGCCAC	This study

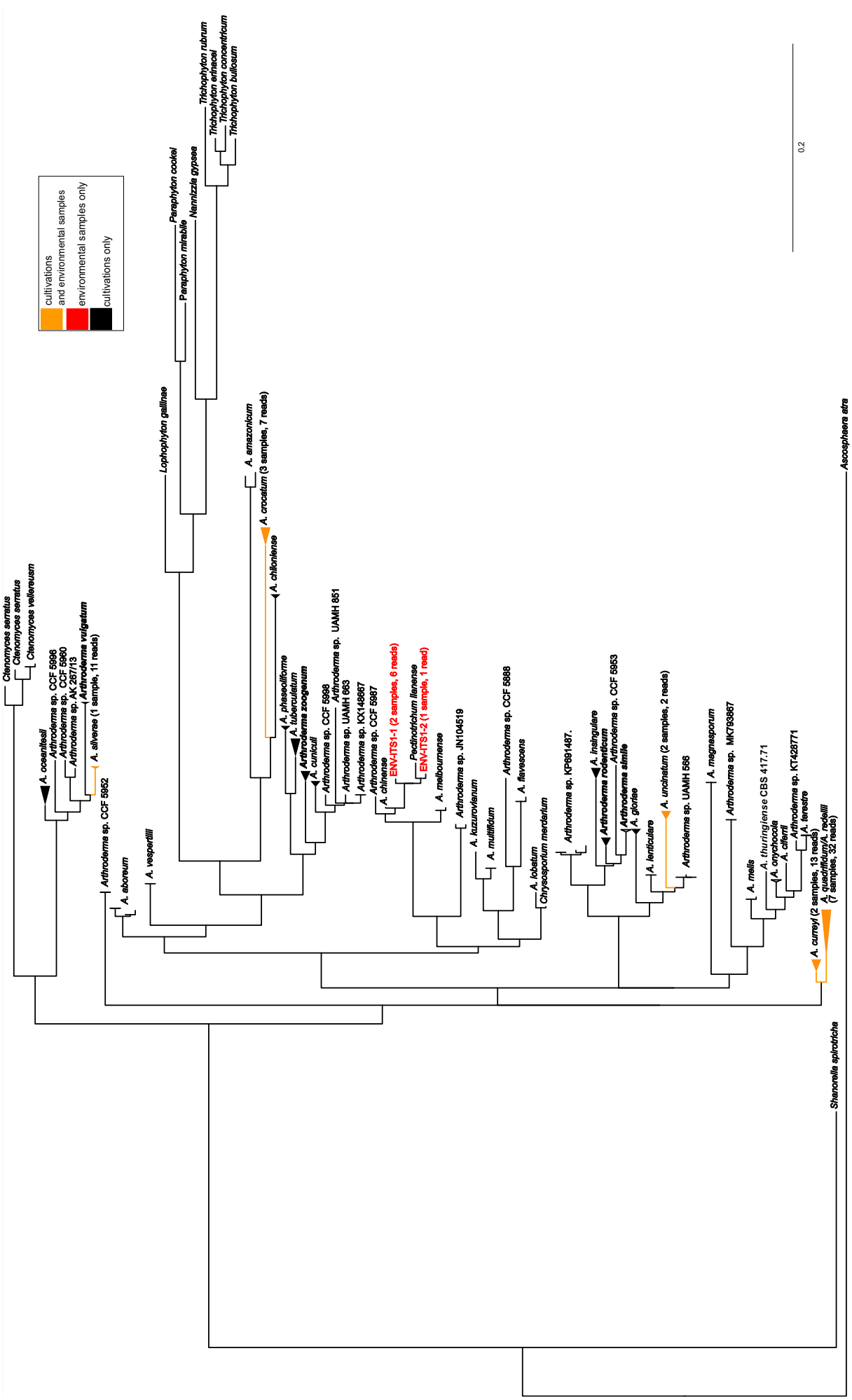

Appendix 2 Phylogenetic relationships among *Arthroderma* strains based on data from NCBI GenBank and the GlobalFungi Database. Data from the GlobalFungi Database include only non-singleton ITS1 sequences (i.e., those presented in the database with at least two reads). The titles of environmental sequences contain the sequence and sample codes taken from the GlobalFungi Database. The terminal clades have been collapsed. The tree was rooted with *Ascosphaera atra*. The branches *Ascosphaera atra* and *Shanorella spirotricha* are shown as one-quarter of the actual length. Phylotypes are differentiated by colours: those obtained from culture-dependent methods are shown in black, those detected by culture-independent methods are shown in red, and those detected by both methodologies are displayed in orange.